Insect Biochemistry and Molecular Biology 165 (2024) 104072

Contents lists available at ScienceDirect

Insect Biochemistry and Molecular Biology

journal homepage: www.elsevier.com/locate/ibmb

From the fat body to the hemolymph: Profiling tick immune and storage proteins through transcriptomics and proteomics

Veronika Urbanová [a], Stephen Lu [b], Eliška Kalinová [c], Larissa Martins [a,d], Tereza Kozelková [a,c], Filip Dyčka [c], José M. Ribeiro [b], Ondřej Hajdušek [a], Jan Perner [a], Petr Kopáček [a,*]

[a] Institute of Parasitology, Biology Centre of the Czech Academy of Sciences, Ceske Budejovice, Czech Republic
[b] Vector Biology Section, Laboratory of Malaria and Vector Research, National Institute of Allergy and Infectious Diseases, Bethesda, MD, USA
[c] Faculty of Science, University of South Bohemia, Ceske Budejovice, Czech Republic
[d] Laboratory of Neurological Infections and Immunity, Rocky Mountain Laboratories - NIH/NIAID, Hamilton, MT, USA

A B S T R A C T

Ticks are blood-feeding arachnids that are known to transmit various pathogenic microorganisms to their hosts. During blood feeding, ticks activate their metabolism and immune system to efficiently utilise nutrients from the host's blood and complete the feeding process. In contrast to insects, in which the fat body is known to be a central organ that controls essential metabolic processes and immune defense mechanisms, the function of the fat body in tick physiology is still relatively unexplored. To fill this gap, we sought to uncover the repertoire of genes expressed in the fat body associated with trachea (FB/Tr) by analyzing the transcriptome of individual, partially fed (previtellogenic) *Ixodes ricinus* females. The resulting catalog of individual mRNA sequences reveals a broad repertoire of transcripts encoding proteins involved in nutrient storage and distribution, as well as components of the tick immune system. To gain a detailed insight into the secretory products of FB/Tr specifically involved in inter-tissue transport and humoral immunity, the transcriptomic data were complemented with the proteome of soluble proteins in the hemolymph of partially fed female ticks. Among these proteins, the hemolipoglyco-carrier proteins were predominant. When comparing immune peptides and proteins from the fat body with those produced by hemocytes, we found that the fat body serves as a unique producer of certain immune components. Finally, time-resolved transcriptional regulation of selected immune transcripts from the FB/Tr was examined in response to experimental challenges with model microbes and analyzed by RT-qPCR. Overall, our data show that the fat body of ticks, similar to insects, is an important metabolic tissue that also plays a remarkable role in immune defense against invading microbes. These findings improve our understanding of tick biology and its impact on the transmission of tick-borne pathogens.

1. Introduction

The fat body (FB) of invertebrates performs a variety of metabolic functions, such as energy metabolism, nutrient management, detoxification processes, and innate immune responses. As such, the FB is commonly considered to be an organ functionally analogous to the liver in vertebrates (Li et al., 2019). Insects store energy reserves in FB cells in the form of glycogen and triglycerides, which form the main component of lipid droplets (LD), the dynamic intracellular lipid storage organelles (Arrese and Soulages, 2010). The FB also synthesizes most hemolymph proteins and circulating metabolites and, along with hemocytes, is the major tissue producing a number of immune molecules (Hetru et al., 2003; Levashina, 2004; Meister and Lagueux, 2003). The insect immune response has been shown to be closely linked to lipid metabolism and biogenesis of LDs (Barletta et al., 2016).

In contrast to insects, the physiological and metabolic functions of the tick (chelicerate) FB remain relatively unexplored. Morphologically, the tick FB is a diffuse tissue closely associated with internal organs, particularly the tracheal trunks. It is also located under the epidermis, near the ovaries and the midgut, the largest organ in the tick body (Denardi et al., 2009; Obenchain and Oliver, 1973). Depending on the location, the FB differs in function and ultrastructure (Coons et al., 1990) and is formed by cells called trophocytes. Nephrocytes, which have been reported in some studies to be closely associated with FB strands and certain areas of the hemocoel, represent a different cell type with a different ultrastructure (Coons et al., 1990; Sonenshine and Roe, 2014).

As in other arthropods, the tick FB has been reported to be involved in metabolism, energy storage, reproduction (especially synthesis of vitellogenin in fully-engorged females), and innate immunity (Coons et al., 1982; Fogaca et al., 2004; Nakajima et al., 2002). However, more detailed studies comparing the specific function of this organ are still pending, and almost nothing is known about immune-related molecules expressed by the FB in ticks. A detailed knowledge of tick immunity is

* Corresponding author.
E-mail address: kopajz@paru.cas.cz (P. Kopáček).

https://doi.org/10.1016/j.ibmb.2024.104072
Received 23 November 2023; Received in revised form 4 January 2024; Accepted 4 January 2024
Available online 5 January 2024

important to understand how pathogens that cause a variety of tick-borne diseases can bypass the tick's innate immunity, survive, and persist in the tick body to eventually be transmitted and infect the vertebrate host (Fogaca et al., 2021; Hajdusek et al., 2013; Sonenshine and Macaluso, 2017). The defense mechanisms in tick, as in other arthropods, consist of two interlinked branches of the cellular and the humoral innate immunity (Eleftherianos et al., 2021; Hillyer, 2016). Cellular defense of ticks is mediated by hemocytes capable to recognize the foreign intruders and eliminate them via phagocytosis, encapsulation, or nodulation (Hajdusek et al., 2013; Kopacek et al., 2010). The humoral response leads to the synthesis/activation of effector molecules that directly destroy pathogens through various mechanisms such as cell lysis or complement-like activities (Hillyer, 2016). Effector molecules of invertebrate immune defenses typically include antimicrobial peptides (AMPs), which are produced primarily in hemocytes and the FB in response to immune activation (Hajdusek et al., 2013; Kumar et al., 2018).

In ticks, there are several classes of AMPs categorized based on their structure, function, and specificity (e.g., defensins, lysozymes, or tick-specific antimicrobial compounds such as microplusin/hebraein) that exhibit a broad spectrum of activity against various microorganisms (Fogaca et al., 2021; Kopacek et al., 2010). Phagocytosis of microbes by tick hemocytes may be coupled with a complement-like system involving thioester-containing proteins (TEPs) and fibrinogen-related lectins (Buresova et al., 2011; Honig Mondekova et al., 2017; Urbanova et al., 2017).

In this study, we performed for the first time, a transcriptomic analysis of the complex of tick FB associated with the trachea (FB/Tr) dissected from four individual, partially fed *Ixodes ricinus* females, the major Lyme disease vector in Europe. The main focus was on the description of transcripts encoding molecules involved in lipid metabolism, storage and transport, as well as molecules possibly involved in tick innate immunity. The transcriptomic analysis was complemented with proteomic analysis of tick hemolymph to determine the proteins synthesized in the FB and secreted into the plasma. Expression of selected FB transcripts encoding immune-related genes was determined in response to an experimental immune challenge using model microbes.

2. Materials and methods

2.1. Biological material

Adult *I. ricinus* females were collected by flagging in a forest near České Budějovice, Czech Republic. Adult females were kept in humid chambers at 24 °C, relative humidity ~95%, and a day/night period of 15/9 h. Females were fed on guinea pigs. All experimental animals were handled in accordance with the Animal Protection Law of the Czech Republic No. 246/1992 Sb., ethics approval No. 25/2020.

2.2. Dissection of fat body-trachea complex

Field-collected *I. ricinus* females were fed on guinea pigs for 5 days and then forcibly removed from their host. All ticks were surface sterilized by washing in 15% ethanol and distilled water (3 × 30s per wash). For library preparation, FB/Tr from four individual females was dissected, placed in 200 μL of cold RNAlater™ (Ambion), immediately frozen in liquid nitrogen, stored at −80 °C, and shipped on dry ice to the North Carolina State Genomic Sciences Laboratory (Raleigh, NC, USA) for Illumina RNA library construction and sequencing as an outsourcing service (see below).

2.3. RNA extraction, library construction and Illumina sequencing

RNA extraction and sequencing library construction were performed as recently described (Medina et al., 2022), and each FB/Tr complex was used for construction of individual library. Briefly, total RNA from FB/Tr was extracted using the Qiagen TissueLyser II and the Qiagen RNA Micro Plus Kit (# 74034). RNA integrity, purity and concentration were assessed using an Agilent 2100 Bioanalyzer with an RNA 6000 Nano Chip (Agilent Technologies, USA). Messenger RNA (mRNA) was purified using the oligo-dT beads provided in the NEBNExt Poly(A) mRNA Magnetic Isolation Module (New England Biolabs, USA) and chemically fragmented and primed with random oligos for first-strand cDNA synthesis. Complementary DNA (cDNA) libraries for Illumina sequencing were constructed using the NEBNext Ultra Directional RNA Library Prep Kit (NEB) and NEBNext Mulitplex Oligos for Illumina (NEB) according to the protocol provided by the manufacturer. The final library size (including adapters) was selected to 300–450 bp using AMPure XP bead isolation (Beckman Coulter, USA). The final quantified libraries were pooled in equimolar amounts for clustering and sequencing on a NovaSeq 6000 DNA sequencer, utilizing an S4, 150 × 2 paired-end sequencing reagent kit (Illumina, USA). The Real-Time Analysis (RTA) software package was used to generate raw base call files (bcl), which were then de-multiplexed by sample into fastq files for data delivery.

2.4. Illumina data analysis

Reads from four FB/Tr complex libraries of *I. ricinus* were trimmed of the Illumina adapters and low-quality sequences (Q < 20) using Trimgalore (https://github.com/FelixKrueger/TrimGalore) and merged into a single file. *De novo* assembly was carried out using Abyss (V2.3.1) (Simpson et al., 2009) with k-values ranging from 25 to 95 (increments of 10) in a single strand mode and Trinity (V2.9.0) (Grabherr et al., 2011). The assemblies from Abyss and Trinity were merged and sequences with at least 95% identity were consolidated using the CD-HIT tool (Fu et al., 2012). The coding DNA sequences (CDS) with an open reading frame (ORF) larger than 200 nucleotides were extracted based on BLAST results to a subset of the Non-redundant (NR), Transcriptome Shotgun Assembly (TSA), and RefSeq-invertebrate databases if they represented coverage of 70% or more to a matching protein. ORFs starting with a methionine and at least 40 amino acids in length were submitted to the signal program (V 3.0) (Bendtsen et al., 2004). Fragments that presented a putative signal peptide were mapped back to the ORFs. To inspect the quality of our *de novo* assembly and CDS extraction strategy, we used the benchmark of universal single-copy orthologs (BUSCO) (Seppey et al., 2019) with the Arachnida database. Relative quantification of each CDS was estimated using the transcript per million (TPM) parameter by mapping the trimmed Illumina reads to the extracted CDS using the RSEM tool (Li and Dewey, 2011). For functional annotation we selected CDS that showed an average TPM ≥3 and were in at least three of the four libraries. Functional classes were attributed to each CDS by an in-house tool that scans a vocabulary (~400 words) and their order of appearance in the protein matches from the BLAST results against several databases (Uniprot, RefSeq-vertebrate, RefSeq-invertebrate, RefSeq-protozoa, CDD, MEROPS, PFAM, Smart, a subset of the NR and TSA), including their similarities and coverage. The annotated CDS were exported to a windows-compatible hyperlinked Excel file available for download (see Data availability below).

2.5. Phylogenetic analysis

Selected peptide sequences (Supplementary Table 1, column I) were searched with BioEdit (version 7.2.5.) using the local BlastP tool against an in-house created compilation of *I. ricinus* tissue transcriptomes (first version deposited) available at the end of 2022 (Iric-pept-NCBI-2022.fas, available upon request). Orthologs of immunoproteins from other invertebrate species were selected based on available literature data. Multiple sequence alignments were performed using the programs Clustal Omega (1.2.2.) and corresponding cladograms created using FastTree (2.1.11), respectively, contained in the Geneious Prime® (20.2.2.) software package.

2.6. Microscopy

The FB/Tr was dissected from partially fed (five days) *I. ricinus* females. For Nomarski and fluorescence microscopy (staining of lipid droplets), samples were fixed in 4% paraformaldehyde and washed in phosphate-buffered saline (PBS) for 3 × 5 min. For Nomarski contrast, samples were embedded in Dabco embedding medium (Sigma) and examined under a motorized Z-Drive BX 63 Olympus microscope with DP74 camera.

To stain the lipid droplets, the tissues were incubated with an LD540 dye (Enamine). For a stock solution, LD540 was dissolved in ethanol (0.5 mg/mL) and then the fixed tissues were incubated with a solution of 0.05 μg/mL LD540 dye in PBS for 30 min and then washed three times with PBS. Nuclei were counterstained with DAPI for 10 min, washed twice with PBS, and mounted in Dabco medium. Dissected FB/Tr was examined under an Olympus FV3000 confocal microscope (405 nm and 514 nm lasers were used for excitation of DAPI and LD540 dye, respectively).

For scanning electron microscopy (SEM) techniques, FB/Tr was fixed in 2.5% glutaraldehyde in phosphate-glucose buffer (PGB, 0.1M sodium phosphate, pH 7.2, 4% w/v glucose) for 24 h and rinsed with PGB (3 × 15 min). After fixation, samples were treated with 2% OsO_4 for 2 h at room temperature. After washing in PGB, the samples were dehydrated in a graded (30–100%) acetone series for 15 min each, dried at the critical point (CPD2 Pelco TM), and gold-plated using a Baltec SCD 050 sputter coater. Samples were analyzed in a JSM 7401F JOEL scanning electron microscope.

2.7. Immune challenge, RNA isolation and quantitative real-time PCR

Ixodes ricinus females were fed on guinea pigs for five days and then divided into five groups (each group contained 5 females). Females were washed in 15% ethanol and distilled water. *Micrococcus luteus* (CIP A270) and *Escherichia coli* (1106) were cultured in LB medium without antibiotics in an orbital shaker at 37 °C. The yeast *Candida albicans* (MDM8) was cultured in Sabouraud medium at 28 °C overnight. After culturing, all microbes were centrifuged (3500×*g*, 10 min), washed twice with sterile PBS, and diluted to an OD 600 = 1. A volume of 69 nL of the microbial suspension or sterile PBS (PBS injection control) was injected with a microinjector (Nanoject II Drummond®) into the hemocoel through to the third coxae of partially fed *I. ricinus* females (field-collected ticks). The other control group were non-injected ticks (NI). The injected females were allowed to rest at room temperature for 6, 24, or 48 h. The complex of FB/Tr was then dissected from females and total RNA was extracted using the NucleoSpin® RNA Kit (Macherey-Nagel, USA) according to the manufacturer's instructions. The concentration was determined using a NanoDrop-1000 spectrophotometer (Thermo Scientific, USA), and 1 μg of total RNA was transcribed into cDNA using the High Fidelity cDNA Synthesis Transcriptor Kit (Roche®). The synthesized cDNA was diluted 20 times in PCR water (Top-Bio). Expression of selected genes in biological samples was quantified by quantitative real-time PCR (RT-qPCR) using QuantStudio 6 Flex (Applied Biosystems®) and gene-specific primers (Supplementary Table 2). The RT-qPCR reactions were performed in technical triplicates in a final volume of 10 μL and contained 5 μL of the 2 × Power SYBR Green Master Mix (Roche), 0.5 μL of the 10 μM mixture of each forward and reverse primers, 2 μL of cDNA, and 2 μL of nuclease-free H_2O. The relative expression of selected genes was normalized to elongation factor 1α (ef-1) (Nijhof et al., 2009), using the mathematical model of (Pfaffl, 2001). Gene-specific primers suitable for unambiguous PCR confirmation of genes expressed in the FB/Tr complex were designed using Primer3 software.

2.8. Proteomic analysis of tick hemolymph

For proteomic analysis of tick hemolymph, adult *I. ricinus* females (field-collected) were fed on guinea pigs for 5 days and then forcibly removed from the host, washed three times with 15 % ethanol and then with distilled water. Hemolymph was collected from the cut leg (10 females per group, 3 groups in total) under a stereomicroscope into 40 μL of chilled sterile PBS. Plasma and hemocytes were separated by centrifugation at 1800 rpm for 5 min at 4 °C. The supernatant (plasma diluted in PBS) was transferred to a clean tube and again spun down at 2500 rpm for 5 min. Pellets (hemocytes) and supernatants (plasma) were stored at −80 °C until further use for proteomic analysis. Hemocyte pellets were homogenized in 200 μL of 50 mM Na-phosphate buffer, pH 7.5, supplemented with 7 M urea, 2 M thiourea, 2% CHAPS, and Halt™ protease inhibitors (Thermo Fisher Scientific, 78439) and processed as previously described (Kozelková et al., 2023). Ten micrograms of plasma or hemocyte homogenate proteins were digested in solution with trypsin, purified with Stage tips solid-phase C18 disc (Empore), and subjected to NanoLS ESI/MS/MS analysis performed on an UltiMate™ 3000 RSLCnano system (Thermo Fisher Scientific) coupled online to the timsTOF Pro mass spectrometer (Bruker Daltonics) as described (Kozelková et al., 2023). Data analysis was performed using MaxQuant software (version 1.6.14) with the integrated search engine Andromeda (Cox and Mann, 2008), using the *I. ricinus* database available in Uniprot (08. 06. 2021) and the contaminant database included in MaxQuant software for protein identification. Data analysis parameters and algorithms for Label-Free Quantification (LFQ) were applied as described (Kozelková et al., 2023). Contaminants, proteins identified by only one peptide with a score of less than 40, and proteins present in only one of three replicate samples were excluded from further analysis. LFQ intensity values were transformed with log2. Two-sample t-tests, principal component analysis, and hierarchical clustering were performed using algorithms integrated in Perseus.

2.9. Statistical analysis

All statistics were performed with GraphPad Prism (version 6.00 for Windows, GraphPad Software San Diego, CA, USA). Expression of selected genes after microbial challenge was compared with the injection control and analyzed using the non-parametric Mann-Whitney test. * = $p < 0.05$, ** = $p < 0.01$, *** = $p < 0.001$.

2.10. Data availability

Transcriptome data was deposited to the National Institute for Biotechnology Information (NCBI) under Bioproject PRJNA748353 and Biosample SAMN20164003. The raw reads were deposited to the Short Reads Archives (SRA) under accession number SRS9601499 and the CDS were deposited with the Transcriptome Shotgun Assembly (TSA) under accession number GJLL000000.2. Supplementary Table 1 can be downloaded from the following link:

https://proj-bip-prod-publicread.s3.amazonaws.com/transcriptome/Iricinus/I_ricinus_fatbody_2022/IR_FB.zip.

The mass spectrometry proteomics data from tick hemolymph were deposited to the ProteomeXchange Consortium via the PRIDE partner repository PXD047619 (Username: reviewer_pxd047619@ebi.ac.uk; Password: eYhRkRXl).

3. Results and discussion

3.1. Description of the fat body transcriptome in partially fed I. ricinus females

The FB cells of *I. ricinus* are closely associated with the tracheal trunks, as shown by light microscopy with Nomarski contrast (Fig. 1A) or scanning electron microscopy (SEM) (Fig. 1B). A similar diffuse localization of FB-forming cell strands around the tracheal trunks was previously demonstrated for partially fed *Amblyomma cajennense* and *I. ricinus* females (Denardi et al., 2009; Urbanova et al., 2015a). For our

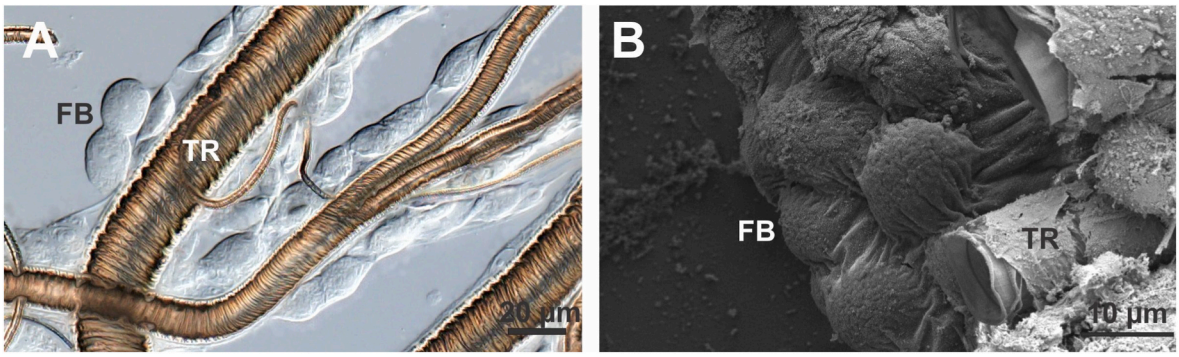

Fig. 1. Fat body/trachea complex from partially fed (5 days of feeding) *I. ricinus* females. A – Light microscopy with Nomarski contrast; B – Scanning electron microscopy. FB – fat body, TR – trachea.

transcriptomic analysis, we used the FB/Tr, as shown in Fig. 1A.

Illumina sequencing of four libraries of FB/Tr complexes dissected from individual partially fed *I. ricinus* females yielded 53,718,335 high-quality sequences. Following *de novo* assembly and CDS extraction, we identified 31,328 putative CDS, exhibiting either a putative signal peptide or high similarity to previously deposited sequences. To evaluate the dataset's quality, we conducted a BUSCO analysis using the Arachnida database as reference, revealing a completeness of 84.7% (72.4% single, 12.3% duplicate), 14.1% missing and 1.2% fragmented, consistent with prior tick transcriptome studies (Lu et al., 2023; Tirloni et al., 2020). When mapping the trimmed Illumina reads to the putative CDS, we obtained similar alignment rates across the four biological replicates (31.8% ± 0.9%). The unmapped reads likely originated from the 5′ and 3′ UTRs that are removed during CDS extraction, from potential non-coding RNA or CDS that were not extracted due to the absence of a putative signal peptide, low similarities to previous deposited sequences, or presented an open reading frame (ORF) with less than 200 nucleotides. Nevertheless, the consistent mapping rates of our samples, in addition to its overall completeness, reflect the quality of the current dataset and the absence of major bias in our samples.

3.2. Functional annotation

For functional annotation, we extracted the putative CDS that were present in at least three of the four biological samples, with an average TPM ≥3. This filtering process resulted in a final list of 8,787 putative transcripts, categorized into 25 functional classes (Fig. 2A, Supplementary Table 1). In the current analysis, the four most abundant functional classes were the "unknown" (26.8% ± 1.1%), "secreted" (18.6% ± 1.5), "protein synthesis" (9.5% ± 0.5%) and "storage" (7.8% ± 1.1%).

In our classification strategy, the "unknown" class encompassed transcripts that exhibit low similarity to previously deposited sequences, and therefore can be considered potential novel sequences, or have a high similarity to sequences of unknown function. This substantial representation underscores our limited knowledge of the protein composition and function of tick FB/Tr, emphasizing the need for further studies in this area. The second most abundant functional class, "secreted", comprised putative secreted proteins commonly found in the salivary glands of blood-feeding arthropods, including mucins, antigen 5-like proteins, lipocalins, esterases, lipases, peptidases, and peptidase inhibitors (Kotsyfakis et al., 2015b; Perner et al., 2018; Schwarz et al., 2014). In the "storage" class, numerous transcripts encoded putative hemelipoglyco-carrier proteins (HeLps) and vitellogenin-like proteins

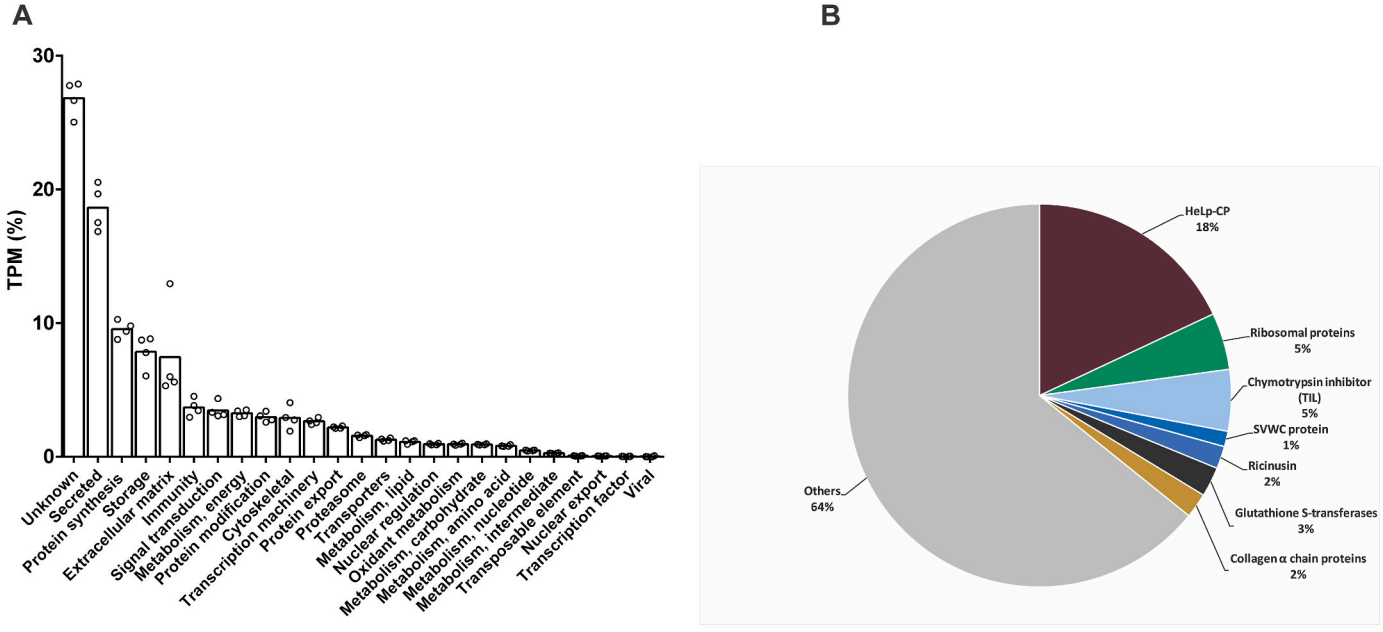

Fig. 2. Functional classification of the 8,787 CDS identified in the *I. ricinus* fat body transcriptome and the most abundant transcripts. A – Bars represent the average TPM (%) of each functional group while the dots represent the TPM (%) observed in each library; B – The most abundant transcripts from different functional groups.

(Supplementary Table 1) that altogether represented about 18% TPM of the total FB/Tr transcriptome (Fig. 2B). This observation aligns with the well established role of the tick FB as the primary site for the production of such proteins (Khalil et al., 2011; Perner et al., 2016a). Notably, among the classes of interest, the "immunity" class was relatively less represented (3.7% ± 0.6%). Nevertheless, it is recognized that the tick FB plays a significant role in the immune response, and in the absence of immunological challenge, genes responsible for the immune response might be expressed at low levels. Finally, our data and functional annotation provide a foundational understanding of the composition of *I. ricinus* FB/Tr. In the subsequent sections, we will delve into a detailed discussion of specific protein families and their potential role in *I. ricinus* physiology.

3.2.1. Lipid metabolism and intracellular storage

The FB serves as a primary site for the storage of energy in the forms of glycogen and lipids (Azeez et al., 2014). The abundant transcripts encoding proteins involved in lipid metabolism are listed in Table 1. Fat body lipids are stored in the form of lipid droplets (LD), multifunctional and highly dynamic intracellular organelles that play a physiological role in packaging and managing the body's fat reserves (Toprak et al., 2020). The main components of LD are triglycerides and cholesterol esters surrounded by phospholipids (Arrese and Soulages, 2010). The staining of LDs with the dye LD540 in the FB cells of *I. ricinus,* and their visualization under the confocal microscope, is shown in Fig. 3. The most abundant structural proteins found exclusively in LDs were perilipins (PLIN), which have been well characterized in mammalian LDs and shown to play an important role in the regulation of lipid metabolism in LDs (Walther et al., 2017). Two transcripts encoding **perilipins** (Irseq_97933, Irseq_11718) were identified in the transcriptome of the tick FB/Tr. The *Drosophila* genome also contains two genes encoding two different PLINs: Lipid Storage Droplet 1/Perilipin 1 (LSD1/PLIN1) and Lipid Storage Droplet 2/Perilipin 2 (LSD2/PLIN2). Both LSD1 and LSD2 are mainly expressed in the FB. It has been shown that lipolysis in the FB adipocytes of the tobacco hornworm *Manduca sexta* is controlled by activation of LD. This occurs through hormonally regulated phosphorylation of LSD1/PLIN1 by protein kinase A, which activates triglyceride lipase (TGL) (Patel et al., 2005). Therefore, LSD1/PLIN1 was thought to be the major player in the activation of lipolysis in insects, whereas LSD2/PLIN2 was reported to induce lipid accumulation in LDs (Arrese and Soulages, 2010; Arrese et al., 2008). Whether tick perilipins play a similar role in lipid storage in LDs and their recruitment remains to be investigated.

Among the FB/Tr transcripts encoding lipolytic enzymes, the most frequently expressed transcripts (Irseq_64848 and Irseq_2932) encoded lipases belonging to the **phospholipase A2** (PLA) group VI (Table 1). PLA2 has been shown to hydrolyze a fatty acid from the sn-2 position of dietary phospholipids in the midgut of mosquito larvae, generating free fatty acids and lysophospholipids to meet their essential nutrient requirements. The second major PLA2 activity contributes to the digestion of neutral lipids from the diet (Abdul Rahim et al., 2018). The transcripts encoding putative **phospholipases B** (PLB) (Irseq_69403, Irseq_69399) were also quite abundant in the FB/Tr transcriptome, but their function is poorly understood. In general, phospholipases B can cleave acyl esters at sn1 or sn2 positions in phospholipids as well as in lysophospholipids (Wilton and Waite, 2002; Zhang and Du, 2021). In addition to these two groups of phospholipases, other transcripts encoding a variety of lipolytic enzymes of different classes were identified and are relatively highly expressed in the transcriptome of the tick FB/Tr (Table 1). For lipid synthesis and LD biogenesis, we identified two highly abundant transcripts encoding enzymes involved in lipid synthesis, namely **fatty acid synthase** (Irseq_2747) and **putative long-chain acyl-coa**

Table 1
Overview of transcripts encoding proteins involved in lipid metabolism.

Group	FB Contig ID	Av TPM	GenBank Protein[a] Identity (%)	Automated annotation	Best match NCBI BlastP (NCBI Access.No)[b]
Lipid storage (perilipins)	Irseq_97933	22.0	MBK3721575 (100%)	put. lipid storage - perilipin 1	adipophilin/perilipin, putative [I. scapularis] (EEC16419.1)
	Irseq_11718	20.0	MBK3721285 (100%)	put.lipid storage - perilipin 2	lipid storage droplets surface-binding protein 2 [I. scapularis] (XP_029845116.2)
Lipases	Irseq_64848	266.0	MBK3721286 (98%)	put. phosphatidylcholine-sterol o-acyltransferase	phospholipase A2 group XV [I. scapularis] (XP_029837760.2)
	Irseq_2932	225.0	JAB69283 (100%)	put. pla2 bee venom like a sub-family of phospholipase a2	phospholipase A2 group XV [I. scapularis] (XP_029837760.2)
	Irseq_69403	114.0	MBK3726301 (94%)	put. phospholipase B-like 2 isoform X1	put. phospholipase B-like 2 isoform X1 (XP_040069484.1)
	Irseq_69399	76.0	JAB78066 (88%)	put. phospholipase B-like 2 isoform X2	put. phospholipase B-like 2 isoform X2 [I. scapularis] (XP_042146951.1)
	Irseq_4841	59.7	MXU97378 (95%)	put. conserved secreted protein precursor	isatin hydrolase-like [I. scapularis] (XP_040068109.1)
	Irseq_70481	44.0	JAA70213 (100%)	put. Group XII secretory phospholipase A2 precursor	group XIIA secretory phospholipase A2-like [I. scapularis] (XP_042144392.1)
	Irseq_76515	31.5	JAB71581 (99%)	put. triglyceride lipase-cholesterol esterase	gastric triacylglycerol lipase [I. scapularis] (XP_040069875.1)
	Irseq_68387	28.6	MBK3723716 (99%)	put. monoacylglycerol lipase abhd12-like protein	lysophosphatidylserine lipase ABHD12 [I. scapularis] (XP_040068315.1)
	Irseq_63174	18.6	MBK3721139 (99%)	put. pogo family transposase, partial	lysophospholipase D GDPD1 isoform X2 [I. scapularis] (XP_040072144.1)
	Irseq_81986	15.2	JAR89929.1 (98%)	put. sn1-specific diacylglycerol lipase alpha	diacylglycerol lipase-alpha isoform X1 [I. scapularis] (XP_040062662.2)
	Irseq_56357	12.0	MXV00640 (99%)	put. hormone-sensitive lipase hsl, partial	hormone-sensitive lipase [I. scapularis] (XP_029843848.3)
	Irseq_92789	8.5	JAP71173 (100%)	put. abhydrolase domain-containing protein	(Lyso)-N-acylphosphatidyl-ethanolamine lipase [I. scapularis] (XP_040357087.1)
	Irseq_18440	8.1	JAB69088 (97%)	put. pancreatic lipase-like enzyme	inactive pancreatic lipase-related protein 1-like [I. scapularis] (XP_029851410.2)
Lipid synthesis	Irseq_2747	518.0	JAB75804 (99%)	put. animal-type fatty acid synthase	fatty acid synthase [I. scapularis] (XP_040077111.1)
	Irseq_35639	244.0	JAP71935 (100%)	put. long-chain acyl-coa synthetase amp-forming, partial	long chain fatty acid CoA ligase, put. [I. scapularis] (EEC06680.1)

Table legend: Contig identification number in FB/Tr transcriptome. Av TPM– Average of four TPM values.
[a] Best match using local BlastP against compilation of *Ixodes ricinus* transcriptomes (Iric-pept-NCBI-2022.fas).
[b] Best match using BlastP search in NCBI for *Ixodida*.

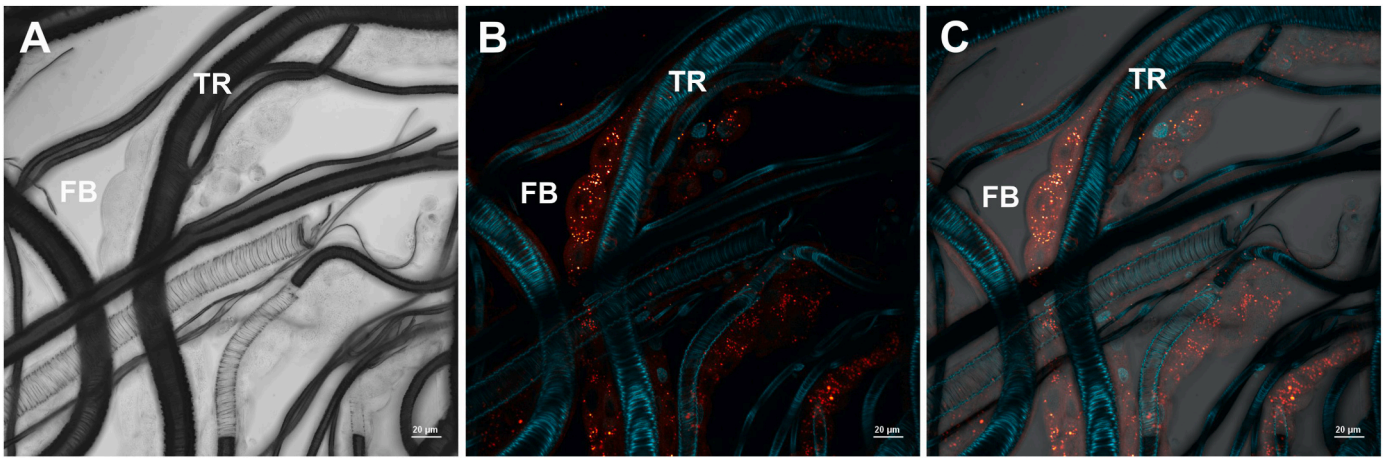

Fig. 3. Lipid droplets staining in fat body cells from partially fed *I. ricinus* females. A – Nomarski contrast; B – lipid droplets staining with LD540 dye (red/yellow); C – merged A and B. The nuclei are counterstained with DAPI (cyan). FB – fat body, TR – trachea.

synthetase (Irseq_35639) (Table 1). We hypothesize that the synthesis of triglyceride molecules, their storage in LD, and their subsequent hydrolysis from FB by adult female ticks mainly meet the energy requirements associated with massive egg production and reproduction.

3.2.2. *Metabolism of sphingolipids*

In addition to the production of triglyceride lipids, the transcriptome of the tick FB/Tr also contained a number of transcripts encoding the biosynthesis and degradation of sphingolipids such as ceramide (Table 2). Sphingolipids are structural components of cell membranes and play an important role as second messengers regulating apoptosis, survival, and differentiation (Acharya and Acharya, 2005; Bauer et al., 2009). In contrast to mammals, in which systemic accumulation of ceramides is a hallmark of nutritional overload associated with a range of pathological processes (Nicholson et al., 2022), we hypothesize that maintenance of sphingolipid homeostasis is vital for ticks given their nutritional overload of blood. **Serine palmitoyltransferase**, **ceramide synthase**, and **sphingolipid desaturase** are the key enzymes involved in ceramide biosynthesis (Kraut, 2011), and the corresponding transcripts (Irseq_100447, Irseq_63061, and Irseq_20158, respectively) were abundant in the transcriptome of the tick FB/Tr (Table 2). Ceramide synthases are highly conserved transmembrane proteins (Voelzmann and Bauer, 2011), and in addition to their role in ceramide biosynthesis, the ceramide synthase homolog in *Drosophila* (schlank) has been identified as a fatty acid-inducible transcriptional repressor of lipid metabolism, where schlank mutants exhibited a reduction in storage fat deposited as triacylglycerols in the FB (Bauer et al., 2009; Sociale et al., 2018). Other transcripts encoding enzymes involved in ceramide catabolism (Kraut, 2011), such as acid, neutral, alkaline ceramidases and ceramide kinase (Irseq_20158, Irseq_36972, Irseq_56517, and Irseq_13000, respectively), were also highly expressed transcripts in the FB/Tr transcriptome.

3.3. *Transcripts encoding secreted proteins*

Transcripts encoding secreted proteins with a signal peptide (Supplemental Table 1, column O) were the second most abundant group in the FB/Tr transcriptome. To verify the role of the FB/Tr tissue in the production of proteins secreted into tick plasma, and to distinguish these from proteins produced by hemocytes, we performed label-free quantitative (LFQ) proteomic analysis of hemolymph from partially fed (fed for 5 days) *I. ricinus* females. Hemocytes were separated from plasma by gentle centrifugation (see Materials and Methods section) and analyzed by shotgun proteomics. After the final selection, 417 proteins were identified (Supplementary Table 3). Most proteins were found exclusively in plasma samples (170), whereas 97 proteins were identified only in hemocytes and 150 proteins were present in the whole hemolymph (Fig. 4).

Table 2
Overview of transcripts encoding enzymes involved in metabolism of sphingolipids.

Group	FB Contig ID	Av TPM	GenBank Protein[a] Identity (%)	Automated annotation	Best match NCBI BlastP (NCBI Access.No)[b]
Sphingolipid metabolism	Irseq_100447	160	JAB77045 (100%)	put. serine palmitoyltransferase	serine palmitoyltransferase 2 [I. scapularis] (XP_002414858.1)
	Irseq_63061	166	JAP73997 (99%)	Protein transporter partial	ceramide synthase 1 [I. scapularis] (XP_002403844.2)
	Irseq_65324	40.7	MBK3725002 (100%)	put. fatty acid desaturase	sphingolipid delta(4)-desaturase DES1 [I. scapularis] (XP_002403975.2)
	Irseq_20158	51.4	JAB68592 (99%)	put. n-acylsphingosine amidohydrolase acid ceramidase 1b	acid ceramidase isoform X2 [I. scapularis] (XP_002405171.3)
	Irseq_56517	32.4	JAA66928 (99%)	put. alkaline ceramidase	alkaline ceramidase 3-like [I. scapularis] (XP_042149000.1)
	Irseq_13000	20.7	JAR93717 (99%)	put. sphingosine kinase	ceramide kinase-like [I. scapularis] (XP_042147602.1)
	Irseq_36972	17.7	JAB71114 (100%)	put. ceramidase	neutral ceramidase [I. scapularis] (XP_040061701.1)

Table legend: Contig identification number in FB/Tr transcriptome. Av TPM – Average of four TPM values.
[a] Best match using local BlastP against compilation of *Ixodes ricinus* transcriptomes (Iric-pept-NCBI-2022.fas).
[b] Best match using BlastP search in NCBI for *Ixodida*.

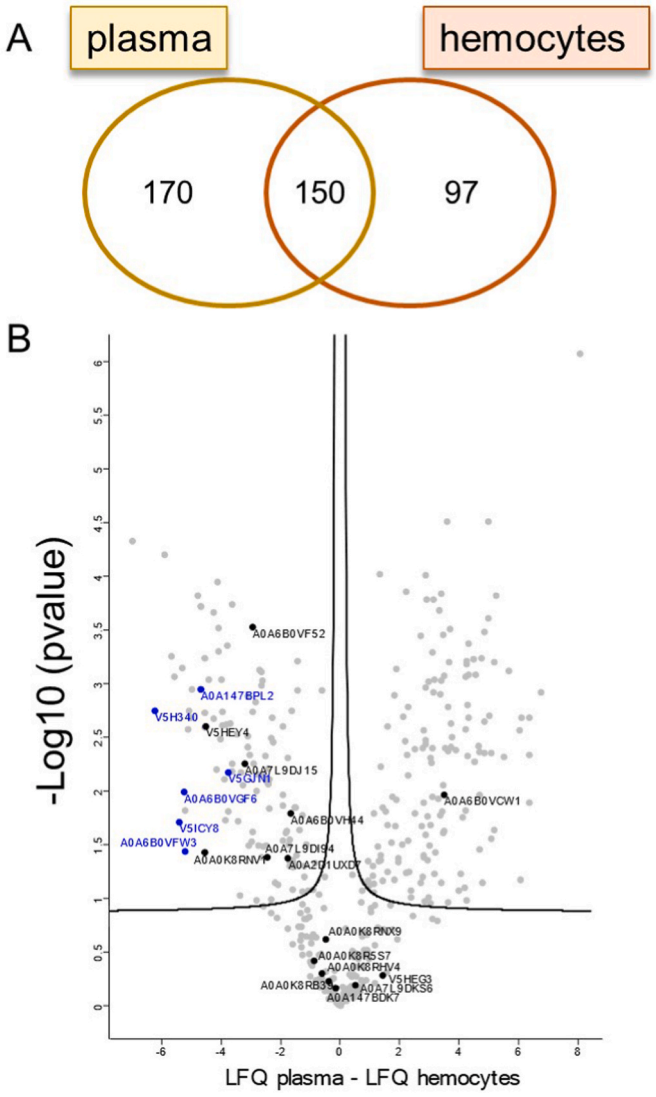

Fig. 4. Overview and distribution of proteins identified in the *I. ricinus* hemolymph proteome. A – Venn diagram of identified proteins in hemolymph samples; B – Two-sided volcano plot of identified proteins. Student's *t*-test, two-sided volcano plot with permutation-based FDR = 0.05 were performed. In blue: HeLp-CP and vitellogenin-related proteins (Table 3); In black: selected immune proteins (Table 4).

3.3.1. *Storage proteins secreted into plasma*

The most expressed transcripts in the FB/Tr transcriptome (Irseq_2443, Irseq_2463, Irseq_2449, Irseq_2471, seqSigP_2446) encoded proteins belonging to the "storage group" and were automatically annotated as **putative vitellogenins** given the presence of the N-terminal Vitellogenin_ N domain aka Lipoprotein N-terminal domain (Table 3). In accord with the high abundance of these transcripts in the FB/Tr transcriptome (Fig. 2B), the corresponding proteins were identified in tick plasma with the highest LFQ values (Supplementary Table 3, sheet 417, column B). Out of these, the most abundant protein, V5GJN1, detected in tick plasma (Table 3 and Supplementary Table 3) was clearly the isoform 3 of the hemelipoglyco-carrier protein (HeLp-CP3, GenBank AJR 36491), which agrees with its previous experimental detection as the major protein component of *I. ricinus* hemolymph (Perner et al., 2016a). These large ~176 kDa HeLp-CPs are known to be major transporters of dietary heme, lipids, and glycans in all developmental stages of ticks, including males (Maya-Monteiro et al., 2000; Perner et al., 2016a; Sonenshine and Roe, 2014). On the other hand, the true yolk vitellogenins, which are transported to the ovaries, are expressed exclusively in fully engorged females during oogenesis (Perner et al., 2016a). In addition to knowledge of stage-specific expression profiles, reliable differentiation of vitellogenins, HeLp-CPs, and other related proteins was made possible by multiple sequence alignment of vitellogenin_N domains (Supplementary Fig. 1) and by creating a corresponding cladogram shown in Fig. 5A. Other distinquishing features of this lipid transfer protein family was the arrangement of the vitellogenin_N, central DUF 1943, and C-terminal von Willebrand factor D domains along the whole molecule and their molecular size (Khalil et al., 2011). Whereas the proteins related to HeLp-CPs consisted of approximately 1,500 amino acid (aa) residues, the true yolk vitellogenins (Vg1 and Vg2) were larger (about 2,000 aa residues(Fig. 5B). As shown by the cladogram (Fig. 5A), two other proteins related to the HeLp-CP group, namely A0A147BPL2, V5H340, and one large protein V5ICY8, consisting of ~3,000 aa residues (presumably an analog of the insect storage protein – apolipohorin), were expressed in the tick FB and secreted into the plasma (Table 3, Fig. 5A and B). Whether these proteins function as heme/lipid transporters, storage proteins or are involved in oogenesis remains to be investigated. Of note, no transcripts encoding the true yolk vitellogenins 1 or 2 were expressed in FB and the corresponding protein products were also not present in the hemolymph of partially fed (previtellogenic) females. This result is consistent with our previous data showing that Vg1 and Vg2 were produced only in fully engorged females during off-host digestion and oogenesis (Perner et al., 2016a).

3.3.2. *Immune molecules expressed in the fat body and secreted into the hemolymph*

Fat body and hemocytes are the major organs of insects and other arthropods that produce immune molecules responsible for defense against invading pathogens and systemic infections. While insect FBs are mainly involved in humoral immunity through the synthesis of effector molecules such as antimicrobial peptides, hemocytes contribute more to cellular immune responses such as phagocytosis (Li et al., 2019; Vaibhvi et al., 2022). Automated functional classification of the filtered transcriptome of *I. ricinus* FB/Tr led to the identification of 141 putative immune genes (Fig. 2A and Supplementary Table 1). In addition, the FB/Tr transcriptome was manually curated to identify transcripts encoding known tick immune proteins of different classes (Fogaca et al., 2021; Kopacek et al., 2010; Sonenshine and Hynes, 2008), resulting in the selection of 20 transcripts listed in Table 4.

3.4. *Functions and immune responses of selected genes*

The experimental design of our transcriptomic and proteomic study necessarily led to the identification of immune transcripts that are constitutively and reproducibly expressed in FB/Tr from partially fed adult females. The Gram(−) bacteria *E. coli*, the Gram(+) bacteria *M. luteus*, and the yeast *C. albicans* are commonly used microbes to study fundamental aspects of the immune system in model organisms such as *Drosophila* (Ferrandon et al., 2007). Accordingly, these model microbes were used in our previous study in which we investigated the role of tick thioester-containing proteins in the phagocytosis by tick hemocytes (Urbanova et al., 2015b). Consistently, *E. coli*, *M. luteus,* and *C. albicans* were used in the current study to examine whether the expression of selected candidate immune genes responded to immune challenge after injection of these model microbes at three-time intervals after injection (6h, 24h, and 48h). The significance of the immune response was compared with the injection of sterile PBS as an injury control. To determine whether proteins synthesized in the tick FB were secreted into the hemolymph, we supplemented our data with semi-quantitative label-free proteomic analysis of plasma and hemocytes, which allowed the identification of proteins preferentially synthesized in the FB rather than in hemocytes (Table 4).

3.4.1. *Highly abundant immune genes*

Two representatives of highly expressed transcripts encoding a

Table 3
Overview of transcripts encoding proteins related to vitellogenins/hemelipoglyco-carrier proteins and their identification in tick hemolymph proteome.

Group	FB Contig ID	Av TPM	GenBank Protein[a] Identity (%)	Automated annotation	Proteome UniProt[b] Identity (%)	LFQ Hemocyte/ Plasma[c]	Best match NCBI BlastP (NCBI Access.No)
Lipid transport	Irseq_2443	38,315.0	JAB70455 (94%)	put. vitellogenin-2	**V5GJN1** (94%)	24.26/28.3	HeLP-CP3 (AJR36491)
	seqSigP-2446	33,510.0	JAB70455 (97%)	put. vitellogenin-2	V5GJN1 (97%)	24.26/28.3	HeLP-CP3 (AJR36491)
	Irseq_2463	25,990.0	MBK3724250 (86%)	put. vitellogenin-2	V5GJN1 (85%)	24.26/28.3	HeLP-CP3 (AJR36491)
	Irseq_2449	8,444.0	MXV01050 (89%)	put. vitellogenin-2	**A0A6B0VFW3** (89%)	19.80/23.32	HeLP-CP3 (AJR36491)
	Irseq_2471	7,234.0	MXV00612 (92%)	put. vitellogenin-2 (frag.)	**A0A6B0VGF6** (92%)	18.62/22.99	HeLP precursor (EEC13578)
	Irseq_29896	278.3	JAB70455(49%)	put. vitellogenin-2	**A0A147BPL2** (100%)	16.37/21.15	vitellogenin-6 [I. scapularis] (XP_029826426.3)
	Irseq_84532	63.4	JAB71606 (100%]	put. vitellogenin-b	**V5ICY8** (100%)	19.31/23.43	uncharact. protein LOC8028815 [I. scapularis] (XP_040070089.2)
	Irseq_15508	5.8	JAB68672 (100%)	put. vitellogenin-1	**V5H340** (98%)	16.78/22.33	vitellogenin-6 [I. scapularis] (XP_029826448.3)

Table legend: Contig identification number in FB/Tr transcriptome. Av TPM – Average of four TPM values.
[a] Best match using local BlastP against compilation of *Ixodes ricinus* transcriptomes (Iric-pept-NCBI-2022.fas).
[b] Best match in UniProt database. In bold – proteins included in the cladogram Fig. 5A and multiple sequence alignment (Supplementary Fig. 1).
[c] Average LFQ values in hemocytes and plasma.

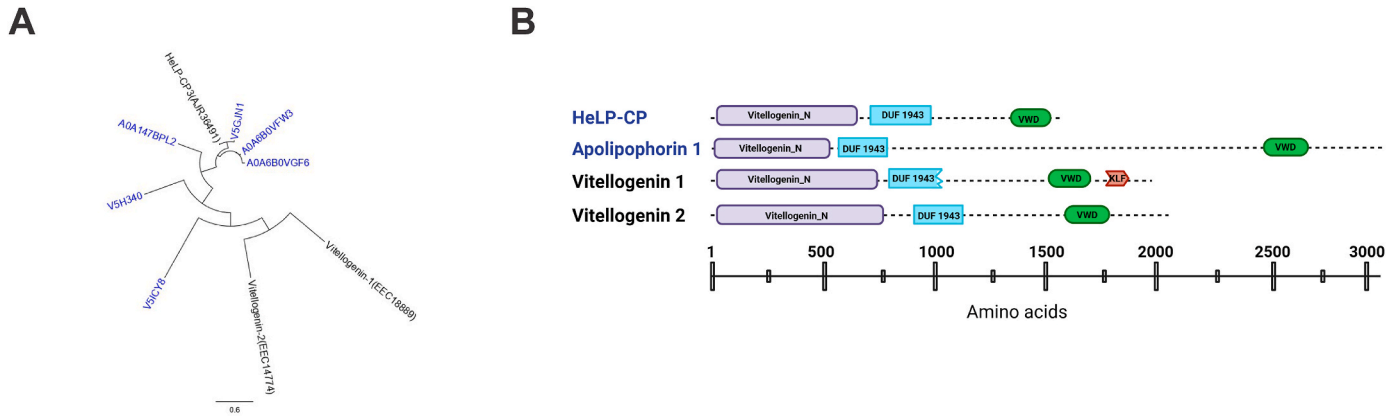

Fig. 5. Recognition of vitellogenin-related proteins identified in the *I. ricinus* hemolymph proteome. A – unrooted cladogram reconstructed using the neighbour joining (NJ) method based on the multiple-sequence alignment of N-terminal vitellogenin_N domains (Supplementary Fig. 1). In blue – Uniprot access nos. of proteins identified in tick hemolymph. In black – protein accession nos. retrieved from the GenBank. Note: no true yolk vitellogenins (Vitellogenin 1 and Vitellogenin 2) were present in the hemolymph of pre-vitellogenic females; B – domain arrangement and molecular size of proteins belonging to tick vitellogenin, HeLp-CP, and apolipohorin family of storage proteins. Domain abbreviations are according to the NCBI conserved domain database (http://www.ncbi.nlm.nih.gov/cdd).

putative **chymotrypsin inhibitor** containing the **TIL (trypsin inhibitor-like) domain** and an 8.9 kDa (**SVWC family**) protein (Fig. 2B) were selected for subsequent RT-qPCR validation (Table 4). The TIL transcript (Irseq_1829) represented a multi-gene family present in a variety of tick tissue transcriptomes and was 84% identical to the TIL domain protein A0A0K8RNV1, which was abundantly present in tick hemolymph (Supplementary Table 3). TIL domain proteins have been reported to have antimicrobial properties in addition to their inhibitory activity (Aguilar-Diaz et al., 2018; Fogaca et al., 2006). Recently, the TIL-domain inhibitor (ACB-TIL) from the Asian corn borer (*Ostrinia furnacalis*) was reported to be involved in the humoral immune responses of this insect pest. The recombinant ACB-TIL has been shown to inhibit hemolymph melanization (prophenoloxidase system) and production of some antimicrobial peptides (Guan et al., 2022). In addition, expression of the transcript encoding ACB-TIL was upregulated after injection of *E. coli* or BmNPV (*Bombyx mori* nuclear polyhedrosis virus) (Guan et al., 2022). Our challenge experiments showed no immune response of the Irseq_1829 transcript (Table 5) and (Supplementary Fig. 2) after microbial challenge. On the other hand, we cannot exclude the possibility that another member of the TIL domain chymotrypsin inhibitor family could be involved in the humoral immunity of ticks.

The SVWC (single-domain von Willebrand factor type C) transcript (SeqSigP-126925) encoded a corresponding 8.9 kDa protein (V5HEY4) found in tick plasma and not in hemocytes (Table 4). These proteins are typically found in arthropods and are thought to be involved in various immune pathways (Sheldon et al., 2007). For example, an SVWC protein from the river shrimp was recently shown to function as an extracellular pattern recognition receptor inducible by bacteria (Qin et al., 2020). However, in our experiments, the expression of this transcript did not respond to microbial challenges (Table 5 and Supplementary Fig. 2).

3.4.2. *Putative immune genes*

Of the other putative immune genes (Table 4), we tested a representative of the **ML-domain** protein family (Irseq_63202), which was closely related to the *I. ricinus* paralog (GeneBank AAP84098), for which immune function has been proposed (Horackova et al., 2010). The encoded ML protein (A0A0K8RNX9) was also synthesized in hemocytes, as shown by the same LFQ values for hemocytes and plasma (Table 4, Supplementary Table 3). An ML protein from the mud crab *Scylla paramamosain* (SpMD2) was recently described as a lipopolysaccharide (LPS)-binding protein that regulates the immune response against Gram (−) bacteria (Wang et al., 2020). Despite this evidence, we did not

Table 4
Overview of selected transcripts encoding immune genes from Fat body-trachea complex.

	FB Contig ID	Protein ID[a]	Av TPM	GenBank Protein[b] (Identity %)	Annotation	Proteome UniProt[c]	LFQ[d] Hemocyte/ Plasma
Abundant	Irseq_1829	MDO4152257	11328	JAB84213 (86%)	TIL-domain protein Put. chymotrypsin inhibitor	A0A0K8RNV1	19.77/22.84
	seqSigP-126925	MDO4148917	13213	JAA70851 (99%)	8.9 kDa protein, SVWC family proteins	V5HEY4	N/19.15
Putative Immune genes	Irseq_63202	MDO4149772	25	MBK3724095 (96%)	ML-domain protein	A0A0K8RNX9	21.20/21.67
	Irseq_63790	MDO4149366	69	JAA71867 (100%)	LPS-induced transcription regulating TNFα (LITAF)	-	-
	Irseq_11954	MDO4148429	32	JAA72427 (94%)	Put. gamma-interferon inducible lysosomal thiol reductase (GILT)	-	-
	Irseq_76499	MDO4145189	117	JAA68616 (97%)	Put. macrophage migration inhibitory factor (MIF Type I)	-	-
	Irseq_71524	MDO4149930	41	MXU99078 (97%)	CLIP-domain SP	A0A6B0VCW1	17.24/N
	Irseq_2155	MDO4150344	606	JAB74946 (99%)	CLIP-domain SP homolog	A0A0K8R5S7	18.50/18.55
AMP	Irseq_99963	MDO4147710	923	JAA71477 (97%)	Defensin-Ir	V5HEG3	21.22/17.82
	Irseq_7363	MDO4149132	16803	MXU92570 (90%)	Ricinusin	A0A0K8RHV4	23.57/24.19
	Irseq_54971	MDO4146878	9	JAA68382 (98%)	Microplusin	A0A0K8RB39	N/15.24
Lectins	Irseq_93341	MDO4151897	13	JAR93712 (98%)	Ixoderin A	-	-
Complement-related	Irseq_2301	MDO4150213	913	QOJ54010 (100%)	Alpha-2-macroglobulin 1 (IrAM-1)	A0A7L9DJ15	20.67/23.87
	Irseq_2740	MDO4146769	788	QOJ54011 (99%)	Alpha-2-macroglobulin 2 (IrAM-2)	A0A6B0VH44	21.53/23.20
	Irseq_7286	MDO4150507	62	QOJ54012 (99%)	Alpha-2-macroglobulin 3 (IrAM-3)	A0A147BDK7	N/15.77
	Irseq_86235	MDO4150665	429	QOJ54014 (98%)	C3-complement component 1 (IrC3-1)	A0A7L9DI94	17.27/19.73
	Irseq_64926	MDO4150664	89	QOJ54015 (99%)	C3-complement component 2 (IrC3-2)	A0A6B0VF52	N/17.83
	Irseq_2599	MDO4150662	55	QOJ54016 (96%)	C3-complement component 3 (IrC3-3)	A0A7L9DKS6	N/14.95
	Irseq_35410	MDO4147310	35	QOJ54018 (100%)	Macroglobulin complement-related (IrMCR-2)	-	-
	Irseq_7589	MDO4147463	319	MXV00447 (94%)	Complement component C2/Bf (IrC2/Bf)	A0A2D1UXD7	15.33/16.73

Table legend: Contig identification number in FB/Tr transcriptome. Av TPM– Average of four TPM values.
[a] Protein Access. No in GenBank.
[b] Best match using local BlastP against compilation of *Ixodes ricinus* transcriptomes (Iric-pept-NCBI-2022.fas) and thioester-containing proteins deposited in GenBank.
[c] Best match in UniProt database.
[d] Average LFQ values in hemocytes and plasma.

observe a response of the transcript encoding the ML-domain protein to the injection of model microbes (Table 5 and Supplementary Fig. 2).

A transcript (Irseq_63790) encoding an **LPS-induced transcription regulating TNFα (LITAF)** was selected based on previous reports showing that LITAF mediates innate immune responses of mice via LPS signaling (Tang et al., 2006). In addition, LITAF homologs have been shown to be involved in the immunity of the mosquito *Anopheles gambiae* to the malarial parasite *Plasmodium* (Smith et al., 2012, 2015). Tick LITAFs are well conserved between different tick species (Supplementary Fig. 3), have no signal peptide, and are predicted to be localized to cellular membranes according to DeepLoc-2.0 (https://services.healthtech.dtu.dk/services/DeepLoc-2.0/). As predicted, LITAF was not found in the proteome of tick hemolymph (Table 4). Consistent with the proposed function, expression of the LITAF homolog of *I. ricinus* responded significantly to injection of Gram(−) *E. coli*, but also to other microbes, especially 24h after injection (a.i.) (Table 5 and Fig. 6). This result warrants a detailed investigation of the role of LITAF in the tick immune system.

Selection of the transcript (Irseq_11954) encoding a **γ-interferon-inducible lysosomal thiol reductase (GILT)** was inspired by literature reports showing that the GILT homolog has an immune function in the hepatopancreas of the red swamp crayfish *Procambarus clarkii*, where it was significantly upregulated after LPS injection (Zhou et al., 2017). In the subsequent study, Pc-GILT expression in crayfish was shown to be responsive not only to LPS but also to peptidoglycan (PGN) and poly I:C treatment, and RNAi-mediated silencing of PcGILT significantly modulated the expression of several immune-related genes (Liu et al., 2019). However, our immune challenge experiment showed no significant differences in the expression of the tick GILT homolog (Irseq_11954) between control ticks and ticks injected with microbes (Table 5 and Supplementary Fig. 2). Despite the presence of a signal peptide indicative of extracellular secretion, the corresponding protein was not identified in tick hemolymph, most likely due to its low levels.

The *I. ricinus* FB/Tr transcript Irseq_76499 encodes a **Macrophage Migration Inhibitory Factor (MIF) type-I** closely related to other orthologs from different tick species. We found no corresponding protein in the plasma or hemocyte proteome, consistent with its predicted cytoplasmic localization. The homologs of mammalian MIFs have been identified and partially characterized in other hard ticks *Amblyomma americanum*, *Haemaphysalis longicornis*, and *Dermacentor variabilis* (Jaworski et al., 2001; Umemiya et al., 2007; Wasala and Jaworski, 2012). MIF was among the first cytokines identified in the early 1960s (Bucala, 2000), but it took nearly four decades for the role of this molecule as a key regulator of innate immunity to be recognized (Calandra and Roger, 2003). The RT-qPCR results of MIF expression in response to microbial challenge showed some minor but significant up-regulation upon injection of *M. luteus* and the yeast *C. albicans* 6h a.i. compared to the injection control. (Table 5 and Fig. 6).

CLIP - domain serine proteases (CLIP-SPs) are nondigestive proteases that contain one or more N-terminal clip domains linked by a linker sequence to a C-terminal trypsin-like serine protease. From our FB/Tr transcriptome, we selected two transcripts encoding an active CLIP-SP (Irseq_71524) with conserved catalytic trypsin triad (H/D/S) and an inactive CLIP-SP homolog (Irseq_2155), in which the serine at the active site was replaced by glycine (CLIPA-type). Based on the TPM-values, the transcript encoding the CLIPA -pseudoprotease was expressed on average about 10-fold more than the active CLIP-SP in the FB/Tr. Accordingly, the active CLIP-SP protein (A0A6B0VCW1) was detected in the hemocyte proteome fraction, indicating that hemocytes and not FB/Tr are the main tissue expressing this pro-enzyme, whereas

Table 5
Overview of the immune responses of selected transcripts to experimental challenge by model microbes.

			6h			24h			48h		
Type	**FB Contig ID**	**Annotation**	*E.c.*	*M.l.*	*C.a.*	*E.c.*	*M.l.*	*C.a.*	*E.c.*	*M.l.*	*C.a.*
Abundant	Irseq_1829	TIL-domain protein Putative chymotrypsin inhibitor									
	seqSigP-126925	8.9 kDa protein, SVWC family proteins									
Putative immune genes	Irseq_63202	ML-domain protein									
	Irseq_63790	LPS-induced transcription regulating TNFα (LITAF)	**		**	**	*	*			
	Irseq_11954	Putative gamma-interferon inducible lysosomal thiol reductase (GILT)									
	Irseq_76499	Putative macrophage migration inhibitory factor (MIF Type I)		*	*						
	Irseq_2155	CLIP-domain SP homolog	*			**					
	Irseq_71524	CLIP-domain SP	***	*							
AMP	Irseq_99963	Defensin-Ir	**	*		**					
	Irseq_7363	Ricinusin									
	Irseq_54971	Microplusin				*			*		
Lectins	Irseq_93341	Ixoderin A				*					
Complement-related	Irseq_2301	Alpha-2-macroglobulin 1 (IrAM-1)				*					
	Irseq_2740	Alpha-2-macroglobulin 2 (IrAM-2)				*					
	Irseq_7286	Alpha-2-macroglobulin 3 (IrAM-3)	*							**	*
	Irseq_86235	C3-complement component 1 (IrC3-1)				**			*		
	Irseq_64926	C3-complement component 2 (IrC3-2)				**		*			
	Irseq_2599	C3-complement component 3 (IrC3-3)				***					
	Irseq_35410	Macroglobulin complement-related (IrMCR-2)	*								
	Irseq_7589	Complement component C2/Bf (IrC2/Bf)				**			*		

Table legend: E.c. – *Escherichia coli*, M.l. – *Micrococcus luteus*, C.a. – *Candida albicans*. Gene expression fold increase in response to microbial injection compared to PBS injection control: 1.2-2 fold; 2.1-3 fold; <3 fold. Asterisks indicate statistically significant differences. * $p<0.05$; ** $p<0.01$; *** $p<0.001$. Data were analyzed by the non-parametric Mann-Whitney test.

the inactive CLIP-SP (A0A0K8R5S7) was equally present in hemocytes and plasma (Table 4). In general, the CLIP-SP enzymes participate in pro-enzyme activation cascades involved in invertebrate humoral defense systems (Cerenius et al., 2010; Kanost and Jiang, 2015). For example, they are involved in hemolymph coagulation in horseshoe crabs (Iwanaga and Lee, 2005; Kawabata and Shibata, 2022; Yamashita et al., 2020), in the activation of pro-phenol oxidase leading to melanization (Cerenius et al., 2008), or in the proteolytic activation of the cytokine Spatzle to form an active Toll ligand leading to synthesis of antimicrobial peptides (Jang et al., 2006).

Multiple sequence alignment with selected members of the invertebrate CLIP-SPs (Supplementary Fig. 4) revealed that the active *I. ricinus* CLIP-SP (Irseq_71524) was closely related to the pro-clotting enzyme from the horseshoe crab *Tachypleus tridentatus* (Muta et al., 1990), activated by the up-stream CLIP-SPs recently tagged as chelicerase B or G (Kawabata and Shibata, 2022). This finding, and our previous characterization of a multi-domain LPS-sensitive serine protease (Urbanova et al., 2015a) related to Limulus factor C, (recently renamed pro-chelicerase C) (Kawabata and Shibata, 2022), suggest that there is indeed some sort of hemolymph coagulation cascade in ticks, although it has not yet been experimentally confirmed. The function of non-active CLIPA-type pseudoproteases in invertebrate immunity is still not fully understood, and they are thought to act as regulators rather than triggers of immune responses (Barillas-Mury, 2007). The CLIPA-SP homolog (Irseq_2155) is related to *Limulus* factor D (Supplementary Fig. 4), which was previously purified from hemocytes of horseshoe crab and showed antimicrobial activity against Gram(−) bacteria (Kawabata et al., 1996). Both of our transcripts (Irseq_71524, Irseq_2155) responded significantly to injection of *E. coli*, and expression of the CLIP-SP also appeared to be upregulated by Gram(+) *M. lutues* 6h a.i. (Table 5 and Fig. 6). Since

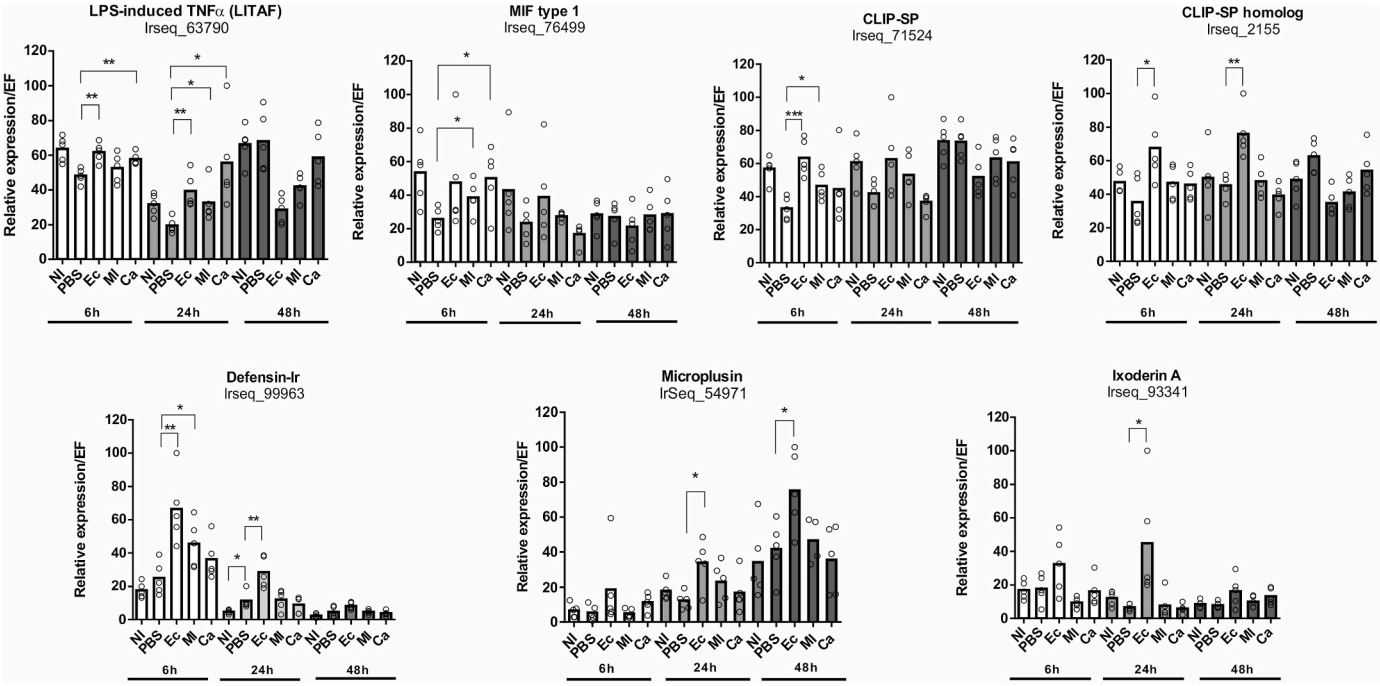

Fig. 6. RT-qPCR analysis of selected immune genes expression in response to aseptic or microbial injection with model microbes. FB/Tr were dissected from partially fed *I. ricinus* females at three time intervals (6h, 24h, and 48h) after microbial injection, sterile PBS injection or from non-injected control. Each group contained FB/Tr from five females and relative gene expression to elongation factor 1α was determined in five independent replicates. *p<0.05, **p<0.01, ***p<0.001. NI – non-injected control; PBS – injury control; Ec – *E. coli*, Ml – *M. luteus*, Ca – *C. albicans*.

ticks do not possess a pro-phenol oxidase-activating system (Fogaca et al., 2021), the exact involvement of CLIP-SPs and their homologs in the innate immune system of ticks need to be systematically investigated.

3.4.3. Antimicrobial peptides

The number of identified transcripts encoding antimicrobial peptides (AMPs), expressed in the FB/Tr of *I. ricinus* females was surprisingly low, likely reflecting the lack of natural immune stimulation in field-collected ticks. Among the most studied effector elements of tick innate immunity are **defensins** (Wu et al., 2022). A type of prepro-defensin from *I. ricinus* (Irseq_99963) was identified in the FB/Tr transcriptome and is closely related to defensins previously tagged as defensin MT3 and/or MT4 (GeneBank AIR77174 and AIR77175, respectively) (Tonk et al., 2014). The corresponding mature defensin V5HEG3 was detected mainly in the hemocyte fraction but also in the plasma (Table 4). The Irseq_99963 transcript and its phylogenetic relationship with other transcripts encoding defensins identified in transcriptomes of *I. ricinus* salivary glands, midgut, or hemocytes (Supplementary Fig. 5) (Kotsyfakis et al., 2015a, 2015b; Perner et al., 2016b) suggest that this defensin was not exclusively FB/Tr-specific. Defensins from *I. ricinus* exert a wide range of antimicrobial activities, mainly targeting the membranes of various Gram(+) bacteria and reportedly attacking Gram(−) bacteria and fungi as well (Tonk et al., 2015). The expression of defensin encoded by Irseq_99963 was upregulated after injection of *E. coli* and *M. luteus* as early as 6h a.i., and the response to *E. coli* remained significantly increased even after 24h a.i. (Table 5 and Fig. 6). To this end, the expression of defensins in the tick FB was reported only for defensin D of the soft tick *Ornithodoros moubata* (Nakajima et al., 2002) and defensin-2 of the hard tick *Dermacentor variabilis* (Ceraul et al., 2007).

Other putative tick-specific antimicrobial peptides are termed **microplusins** after the first representative characterized in *R. microplus* (Fogaca et al., 2004). These cysteine- and histidine-rich proteins exert their bacteriostatic effects against Gram(+) bacteria via chelation of copper ions, which are required for bacterial respiration (Silva et al., 2009). Most transcripts annotated as microplusins in *I. ricinus* FB/Tr were closely related to ricinusin (GenBank ABB79785), which, however, shares little resemblance (only about 35% identity) to the microplusin of *R. microplus,* except for the pattern of conserved cysteine residues (Supplementary Fig. 6). Ricinusin-related transcripts were strongly represented in the FB/Tr transcriptome (e.g., the Irseq_7363 transcript with an average TPM value of 16,803) and accordingly, the encoded protein (A0A0K8RHV4) was among the most abundant proteins identified in tick hemolymph (Table 4 and Supplementary Table 3).

In contrast, the Irseq_54971 transcript, encoding a microplusin homolog more related to that of *R. microplus* (~60% identity), was much less expressed in FB/Tr (average TPM 9.3), and the amount of the corresponding protein (A0A0K8RB39) in tick plasma was also rather low (Table 4). On the other hand, this minor transcript Irseq_54971 responded significantly to injection of *E. coli* at 24h and 48h a.i. (Table 5 and Fig. 6), whereas expression of ricinusin-related Irseq_7363 did not change at all (Table 5 and Supplementary Fig. 2). Thus, the role of ricinusins/microplusins in the immune system of *I. ricinus* remains unclear and awaits future functional studies.

3.4.4. Lectins

From several transcripts that were automatically annotated as putative lectins, e.g., hemolectins, p-selectins, galectins, etc. (Supplementary Table 1), we selected the transcript (Irseq_93341) encoding a fibrinogen-related protein (FREP). Multiple sequence alignment and phylogenetic analysis of this transcript with other FREPs identified in different tissue transcriptomes of *I. ricinus* (Supplementary Fig. 7) clearly showed that it belongs to the **Ixoderin A** group. Ixoderin A is homologous to tachylectins 5A,B from the horseshoe crab (Gokudan et al., 1999) and the hemolymph lectin Dorin M from the soft tick *O. moubata*, for which lectin (sugar binding activity) has been demonstrated (Kovar et al., 2000; Rego et al., 2006). The role of Ixoderin A as a hemolymph lectin was also demonstrated by RNAi-mediated silencing that resulted in elimination of hemaglutination of mice red blood cells (Honig Mondekova et al., 2017). The results of previous tissue expression profiling

showed that the major tissues producing Ixoderin A were hemocytes and Malpighian tubules, while Ixoderin B-related transcripts were exclusively expressed in salivary glands (Honig Mondekova et al., 2017). Expression of the Ixoderin A-encoding transcript in *I. ricinus* FB/Tr responded to injection of *E. coli* 24h a.i. (Table 5 and Fig. 6), but did not appear to be induced solely by sterile PBS injection, as previously shown in whole-body homogenates of *I. ricinus* (Honig Mondekova et al., 2017). The relatively low TPM values obtained for Irseq_93341, and the surprising absence of the corresponding protein in tick hemocytes or plasma, suggest that the expression of Ixoderin A-related isoforms or splice variants may be highly specific for different microbial infections and strictly spatially and temporally controlled.

3.4.5. Components of the tick complement-like system

Nine thioester-containing proteins (TEPs), including three α2-macroglobulins (*Ir*AM-1,2,3), three C3 complement components (*Ir*C3-1,2,3), one insect-type TEP (*Ir*TEP), and two macroglobulin complement-related (MCR) molecules (IrMCR-1,2), have been previously identified and annotated in *I. ricinus* (Buresova et al., 2011; Fogaca et al., 2021; Urbanova et al., 2015b). Our previous tissue expression profiling showed that most tick TEPs were expressed in the tick FB, except for *Ir*MCR-1 and *Ir*TEP, which were specifically expressed in the salivary glands and ovaries, respectively. In agreement with this, seven transcripts were found in the transcriptome of *I. ricinus* FB/Tr (Table 4). Based on the TPM values, the dominant transcripts expressed in FB/Tr were Irseq_2301, Irseq_2740, and Irseq_86235, encoding proteins *Ir*AM1 (A0A7L9DJ15), *Ir*AM2 (A0A6B0VH44), and *Ir*C3-1 (A0A7L9DI94), respectively, that were correspondingly abundantly present in tick plasma (Table 4 and Supplementary Table 3). Experiments with the model microbes showed the strongest expression response of *Ir*C3-1, 2, and 3 to injection of *E.coli* 24h a.i., and of *Ir*C3-1 after 48h a.i. (Table 5 and Fig. 7). Expression of tick α_2-macroglobulins in response to injection of *E. coli* occurred as early as 6h a.i. for *Ir*AM3 and 24h a.i. for *Ir*AM1 and *Ir*AM2. In addition to *E.coli*, *Ir*C3-2 and *Ir*AM3 also responded to the injection of yeast *C. albicans* 24h and 48h a.i., respectively. Our previous study showed the highest response of *Ir*C3-1 to *C. albicans* injection, albeit under different experimental conditions (12h a.i. and RT-qPCR mRNA quantification in the whole body homogenates).

Another characterized component of the *I. ricinus* complement system is the convertase related to complement factors C2 or B, referred to as *Ir*C2/Bf (Urbanova et al., 2018). It is a multidomain molecule consisting of 5–7 complement control protein (CCP) modules (also known as sushi or SCR – short consensus repeats) that are varied by alternative splicing, followed by a von Willebrand factor A domain and a C-terminal trypsin-like domain. The relatively high TPM values of the *Ir*C2/Bf transcript (Irseq_7589) in the FB/Tr transcriptome and the presence of the *Ir*C2/Bf protein (A0A2D1UXD7) in the hemolymph (Table 4, Supplementary Table 3) were consistent with RT-qPCR tissue expression profiles showing that the tick FB is the main tissue producing this molecule (Urbanova et al., 2018). In contrast to the previous study, in which we observed increased expression of *Ir*C2/Bf mRNA in whole-body homogenates after injection of *C. albicans* 12h after challenge, here we observed a statistically significant response to injection of *E. coli* 24h and 48h a.i. (Table 5 and Fig. 7).

3.4.6. Overview of immune responses of selected transcripts to microbial challenges

The overview of the immune responses of 20 selected genes to microbial challenges compared with injection control (PBS), shown in detail in the Supplementary Fig. 2, Fig. 6 and 7 is summarized in Table 5. Expression of selected representatives of the TIL domain inhibitor, 8.9 kDa SVWC, ML domain protein families, the GILT homolog, and the highly expressed ricinusin did not respond to injection of a model microbe. Five transcripts encoding LITAF, MIF type I, CLIP domain SP, defensin Ir, and *Ir*AM-3 responded to *M. luteus* injection at different time points a.i. The majority (fourteen) of transcripts examined (namely LITAF, CLIP domain SP, CLIP domain SP homolog, defensin Ir, microplusin, ixoderin A, *Ir*AM-1,2,3, *Ir*C3-1,2,3, *Ir*MCR-2, and *Ir*FB/C2) were upregulated in response to *E. coli* injection. The most frequent time interval for a significant immune response was 24h a.i., although an early

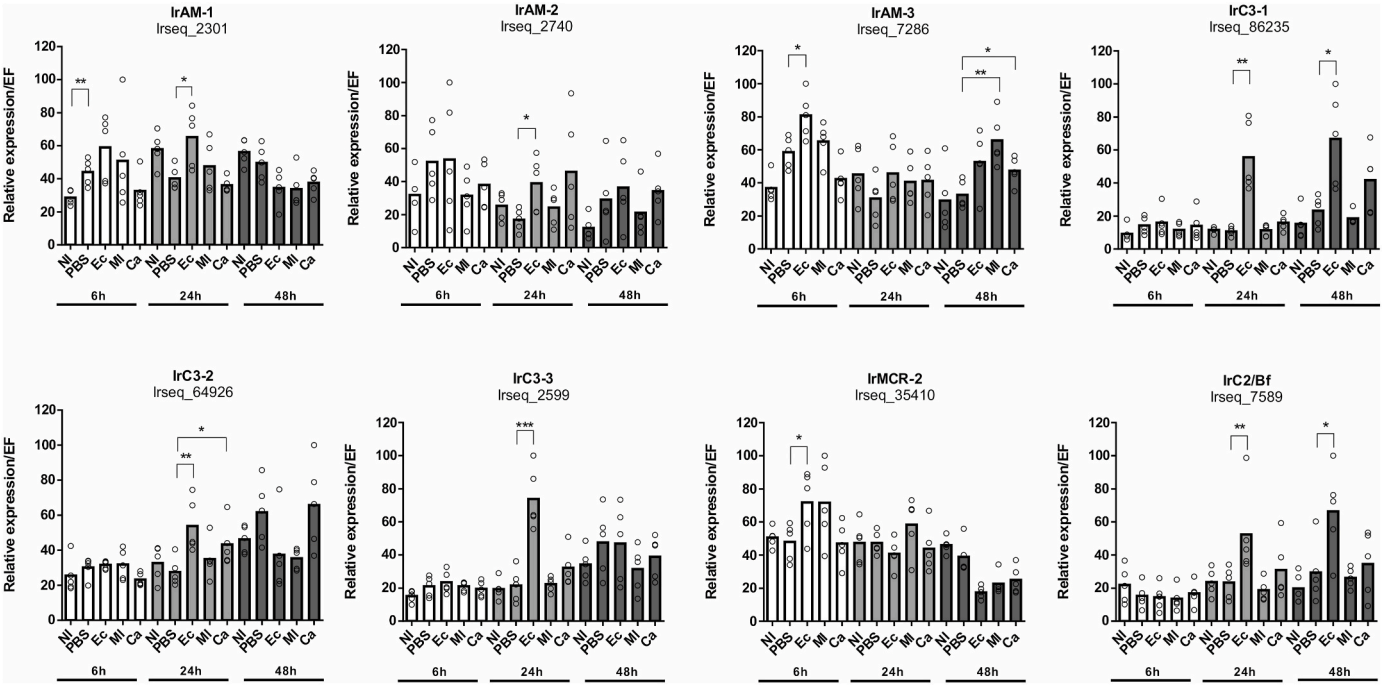

Fig. 7. RT-qPCR analysis of genes encoding tick complement components in response to aseptic or microbial injection with model microbes. FB/Tr were dissected from partially fed *I. ricinus* females at three time intervals (6h, 24h, and 48h) after microbial injection, sterile PBS injection or from non-injected control. Each group contained FB/Tr from five females and relative gene expression to elongation factor 1α was determined in five independent replicates. *p<0.05, **p<0.01, ***p<0.001. NI – non-injected control; PBS – injury control; Ec – *E. coli*, Ml – *M. luteus*, Ca – *C. albicans*.

response was also observed for seven genes 6h a.i. and a late response for four genes 48h a.i. (Table 5).

4. Conclusion

The FB of arthropods is a multifunctional tissue that plays a role in energy homeostasis (adipose tissue) and the immune response (Zhang and Xi, 2014). Studies in model arthropods have shown that FB cells and hemocytes are the only professional immune cells (Vaibhvi et al., 2022). Although both produce AMPs, the FB is mainly responsible for the humoral immune response (Vlisidou and Wood, 2015). This study combines data resulting from the first transcriptomic analysis of the FB and the first hemolymph proteome analysis performed for any tick species. The design of the study was focused on reproducibility of transcripts and encoded proteins expressed in a defined stage, specifically partially fed, field-collected *I. ricinus* females. The collected data thus resulted in a catalog of transcripts/proteins constitutively expressed in the FB and present in the hemolymph of the tick. The semi-quantitative expression data in the FB/Tr transcriptome based on TPM values match well with semi-quantitative LFQ values of protein levels in tick plasma. The most abundant transcripts identified in the FB of the previtellogenic *I. ricinus* females belong to the group of hemolipoglyco-carrier proteins (HeLp-CPs) and, correspondingly, the encoded proteins were highly represented in tick plasma. Among the most abundant transcripts encoding proteins possibly playing a role in tick immunity were identified members of the TIL-domain chymotrypsin inhibitor family as well as ricinusin, distantly related to microplusin from *R. microplus* (Fogaca et al., 2004). Other immune genes produced by the tick FB (e.g., components of tick complement-like system, defensins, fibrinogen-related proteins) appeared to respond to challenge by different microbes. Whether these microbes are specifically recognized by immune signaling pathways (e.g. Toll and/or Imd), and whether the increased secretion of these molecules could impact survival of tick-borne pathogens in the tick hemolymph and their transmission from the tick to the host, should be clarified in following studies.

CRediT authorship contribution statement

Veronika Urbanová: Writing – original draft, Visualization, Methodology, Investigation, Conceptualization. **Stephen Lu:** Writing – original draft, Software, Project administration, Data curation. **Eliška Kalinová:** Validation, Methodology, Data curation. **Larissa Martins:** Software, Methodology, Investigation, Data curation. **Tereza Kozelková:** Writing – original draft, Software, Methodology, Investigation, Data curation. **Filip Dyčka:** Software, Methodology. **José M. Ribeiro:** Software, Formal analysis, Data curation. **Ondřej Hajdušek:** Methodology, Formal analysis. **Jan Perner:** Writing – original draft, Formal analysis, Data curation. **Petr Kopáček:** Writing – original draft, Supervision, Project administration, Funding acquisition, Data curation, Conceptualization.

Data availability

Data availibility paragraph is included in the manuscript

Acknowledgements

This study was mainly supported by the Czech Science Foundation Grant. to. 20-05736S to P.K. Additional support to V.U., T.K., O.H. , J.P. , and P.K. was from the 'Centre for research of pathogenicity and virulence of parasites' (no. CZ.02.1.01/0.0/0.0/16_019/0000759) funded by the European Regional Development Fund (ERDF) and Ministry of Education, Youth, and Sport (MEYS). We thank to Dr. Michalis Kotsyfakis for arranging and organizing NGS sequencing at the North Carolina State Genomic Sciences Laboratory (Raleigh, NC, USA).

Appendix A. Supplementary data

Supplementary data to this article can be found online at https://doi.org/10.1016/j.ibmb.2024.104072.

References

Abdul Rahim, N.A., Othman, M., Sabri, M., Stanley, D.W., 2018. A midgut digestive phospholipase A(2) in larval mosquitoes, *Aedes albopictus* and *Culex quinquefasciatus*. Enzym. Res. 2018, 9703413.

Aguilar-Diaz, H., Esquivel-Velazquez, M., Quiroz-Castaneda, R.E., Miranda-Miranda, E., Conde-Baeye, R.J.P., Cobaxin-Cardenas, M., Ostoa-Saloma, P., Cossio-Bayugar, R., 2018. Comparative hemolymph proteomic and enzymatic analyses of two strains of *Rhipicephalus* (*Boophilus*) *microplus* ticks resistant and susceptible to ixodicides. BioMed Res. Int. 2018, 9451547.

Acharya, U., Acharya, J.K., 2005. Enzymes of sphingolipid metabolism in *Drosophila melanogaster*. Cell. Mol. Life Sci. 62, 128–142.

Arrese, E.L., Rivera, L., Hamada, M., Mirza, S., Hartson, S.D., Weintraub, S., Soulages, J. L., 2008. Function and structure of lipid storage droplet protein 1 studied in lipoprotein complexes. Arch. Biochem. Biophys. 473, 42–47.

Arrese, E.L., Soulages, J.L., 2010. Insect fat body: energy, metabolism, and regulation. Annu. Rev. Entomol. 55, 207–225.

Azeez, O.I., Meintjes, R., Chamunorwa, J.P., 2014. Fat body, fat pad and adipose tissues in invertebrates and vertebrates: the nexus. Lipids Health Dis. 13, 71.

Barillas-Mury, C., 2007. CLIP proteases and *Plasmodium* melanization in *Anopheles gambiae*. Trends Parasitol. 23, 297–299.

Barletta, A.B., Alves, L.R., Silva, M.C., Sim, S., Dimopoulos, G., Liechocki, S., Maya-Monteiro, C.M., Sorgine, M.H., 2016. Emerging role of lipid droplets in *Aedes aegypti* immune response against bacteria and Dengue virus. Sci. Rep. 6, 19928.

Bauer, R., Voelzmann, A., Breiden, B., Schepers, U., Farwanah, H., Hahn, I., Eckardt, F., Sandhoff, K., Hoch, M., 2009. Schlank, a member of the ceramide synthase family controls growth and body fat in *Drosophila*. EMBO J. 28, 3706–3716.

Bendtsen, J.D., Nielsen, H., von Heijne, G., Brunak, S., 2004. Improved prediction of signal peptides: SignalP 3.0. J. Mol. Biol. 340, 783–795.

Bucala, R., 2000. Signal transduction. A most interesting factor. Nature 408, 146–147.

Buresova, V., Hajdusek, O., Franta, Z., Loosova, G., Grunclova, L., Levashina, E.A., Kopacek, P., 2011. Functional genomics of tick thioester-containing proteins reveal the ancient origin of the complement system. J. Innate Immun. 3, 623–630.

Calandra, T., Roger, T., 2003. Macrophage migration inhibitory factor: a regulator of innate immunity. Nat. Rev. Immunol. 3, 791–800.

Ceraul, S.M., Dreher-Lesnick, S.M., Gillespie, J.J., Rahman, M.S., Azad, A.F., 2007. New tick defensin isoform and antimicrobial gene expression in response to *Rickettsia montanensis* challenge. Infect. Immun. 75, 1973–1983.

Cerenius, L., Lee, B.L., Soderhall, K., 2008. The proPO-system: pros and cons for its role in invertebrate immunity. Trends Immunol. 29, 263–271.

Cerenius, L., Kawabata, S., Lee, B.L., Nonaka, M., Soderhall, K., 2010. Proteolytic cascades and their involvement in invertebrate immunity. Trends Biochem. Sci. 35, 575–583.

Coons, L.B., Tarnowski, B., Ourth, D.D., 1982. *Rhipicephalus sanguinius*: localization of vitellogenin synthesis by immunological methods and electron microscopy. Exp. Parasitol. 54, 331–339.

Coons, L.B., L'Amoreaux W, J., Rosell-Davis, R., Starr-Spires, L., 1990. Fine structure of the fat body and nephrocytes in the life-stages of *Dermacentor variabilis*. Exp. Appl. Acarol. 8, 125–142.

Cox, J., Mann, M., 2008. MaxQuant enables high peptide identification rates, individualized p.p.b.-range mass accuracies and proteome-wide protein quantification. Nat. Biotechnol. 26, 1367–1372.

Denardi, S.E., Bechara, G.H., Camargo-Mathias, M.I., 2009. Fat body cells of *Amblyomma cajennense* partially engorged females (Acari: Ixodidae) and their role on vitellogenesis process. Exp. Parasitol. 121, 213–218.

Eleftherianos, I., Heryanto, C., Bassal, T., Zhang, W., Tettamanti, G., Mohamed, A., 2021. Haemocyte-mediated immunity in insects: cells, processes and associated components in the fight against pathogens and parasites. Immunology 164, 401–432.

Ferrandon, D., Imler, J.L., Hetru, C., Hoffmann, J.A., 2007. The *Drosophila* systemic immune response: sensing and signalling during bacterial and fungal infections. Nat. Rev. Immunol. 7, 862–874.

Fogaca, A.C., Lorenzini, D.M., Kaku, L.M., Esteves, E., Bulet, P., Daffre, S., 2004. Cysteine-rich antimicrobial peptides of the cattle tick *Boophilus microplus*: isolation, structural characterization and tissue expression profile. Dev. Comp. Immunol. 28, 191–200.

Fogaca, A.C., Almeida, I.C., Eberlin, M.N., Tanaka, A.S., Bulet, P., Daffre, S., 2006. Ixodidin, a novel antimicrobial peptide from the hemocytes of the cattle tick *Boophilus microplus* with inhibitory activity against serine proteinases. Peptides 27, 667–674.

Fogaca, A.C., Sousa, G., Pavanelo, D.B., Esteves, E., Martins, L.A., Urbanova, V., Kopacek, P., Daffre, S., 2021. Tick immune system: what is known, the interconnections, the gaps, and the challenges. Front. Immunol. 12, 628054.

Fu, L., Niu, B., Zhu, Z., Wu, S., Li, W., 2012. CD-HIT: accelerated for clustering the next-generation sequencing data. Bioinformatics 28, 3150–3152.

Gokudan, S., Muta, T., Tsuda, R., Koori, K., Kawahara, T., Seki, N., Mizunoe, Y., Wai, S. N., Iwanaga, S., Kawabata, S., 1999. Horseshoe crab acetyl group-recognizing lectins involved in innate immunity are structurally related to fibrinogen. Proc. Natl. Acad. Sci. U.S.A. 96, 10086–10091.

Grabherr, M.G., Haas, B.J., Yassour, M., Levin, J.Z., Thompson, D.A., Amit, I., Adiconis, X., Fan, L., Raychowdhury, R., Zeng, Q., Chen, Z., Mauceli, E., Hacohen, N., Gnirke, A., Rhind, N., di Palma, F., Birren, B.W., Nusbaum, C., Lindblad-Toh, K., Friedman, N., Regev, A., 2011. Full-length transcriptome assembly from RNA-Seq data without a reference genome. Nat. Biotechnol. 29, 644–652.

Guan, R., Hu, S., Li, X., An, S., Miao, X., Li, H., 2022. A TIL-type serine protease inhibitor involved in humoral immune response of Asian corn borer *Ostrinia furnaculis*. Front. Immunol. 13, 900129.

Hajdusek, O., Sima, R., Ayllon, N., Jalovecka, M., Perner, J., de la Fuente, J., Kopacek, P., 2013. Interaction of the tick immune system with transmitted pathogens. Front. Cell. Infect. Microbiol. 3, 26.

Hetru, C., Troxler, L., Hoffmann, J.A., 2003. *Drosophila melanogaster* antimicrobial defense. J. Infect. Dis. 187 (Suppl. 2), S327–S334.

Hillyer, J.F., 2016. Insect immunology and hematopoiesis. Dev. Comp. Immunol. 58, 102–118.

Honig Mondekova, H., Sima, R., Urbanova, V., Kovar, V., Rego, R.O.M., Grubhoffer, L., Kopacek, P., Hajdusek, O., 2017. Characterization of *Ixodes ricinus* fibrinogen-related proteins (ixoderins) discloses their function in the tick innate immunity. Front. Cell. Infect. Microbiol. 7, 509.

Horackova, J., Rudenko, N., Golovchenko, M., Havlikova, S., Grubhoffer, L., 2010. IrML - a gene encoding a new member of the ML protein family from the hard tick, *Ixodes ricinus*. J. Vector Ecol. 35, 410–418.

Iwanaga, S., Lee, B.L., 2005. Recent advances in the innate immunity of invertebrate animals. J. Biochem. Mol. Biol. 38, 128–150.

Jang, I.H., Chosa, N., Kim, S.H., Nam, H.J., Lemaitre, B., Ochiai, M., Kambris, Z., Brun, S., Hashimoto, C., Ashida, M., Brey, P.T., Lee, W.J., 2006. A Spatzle-processing enzyme required for toll signaling activation in *Drosophila* innate immunity. Dev. Cell 10, 45–55.

Jaworski, D.C., Jasinskas, A., Metz, C.N., Bucala, R., Barbour, A.G., 2001. Identification and characterization of a homologue of the pro-inflammatory cytokine Macrophage Migration Inhibitory Factor in the tick, *Amblyomma americanum*. Insect Mol. Biol. 10, 323–331.

Kanost, M.R., Jiang, H., 2015. Clip-domain serine proteases as immune factors in insect hemolymph. Curr. Opin. Insect Sci. 11, 47–55.

Kawabata, S., Tokunaga, F., Kugi, Y., Motoyama, S., Miura, Y., Hirata, M., Iwanaga, S., 1996. *Limulus* factor D, a 43-kDa protein isolated from horseshoe crab hemocytes, is a serine protease homologue with antimicrobial activity. FEBS Lett. 398, 146–150.

Kawabata, S.I., Shibata, T., 2022. New insights into the hemolymph coagulation cascade of horseshoe crabs initiated by autocatalytic activation of a lipopolysaccharide-sensitive zymogen. Dev. Comp. Immunol. 135, 104491.

Khalil, S.M., Donohue, K.V., Thompson, D.M., Jeffers, L.A., Ananthapadmanaban, U., Sonenshine, D.E., Mitchell, R.D., Roe, R.M., 2011. Full-length sequence, regulation and developmental studies of a second vitellogenin gene from the American dog tick, *Dermacentor variabilis*. J. Insect Physiol. 57, 400–408.

Kopacek, P., Hajdusek, O., Buresova, V., Daffre, S., 2010. Tick innate immunity. Adv. Exp. Med. Biol. 708, 137–162.

Kotsyfakis, M., Kopacek, P., Franta, Z., Pedra, J.H.F., Ribeiro, J.M.C., 2015a. Deep sequencing analysis of the *Ixodes ricinus* Haemocytome. PLoS Neglected Trop. Dis. 9, e0003754.

Kotsyfakis, M., Schwarz, A., Erhart, J., Ribeiro, J.M., 2015b. Tissue- and time-dependent transcription in *Ixodes ricinus* salivary glands and midguts when blood feeding on the vertebrate host. Sci. Rep. 5, 9103.

Kovar, V., Kopacek, P., Grubhoffer, L., 2000. Isolation and characterization of Dorin M, a lectin from plasma of the soft tick *Ornithodoros moubata*. Insect Biochem. Mol. Biol. 30, 195–205.

Kozelková, T., Dyčka, F., Lu, S., Urbanová, V., Frantová, H., Sojka, D., Šíma, R., Horn, M., Perner, J., Kopáček, P., 2023. Insight into the dynamics of the *Ixodes ricinus* nymphal midgut proteome. Mol. Cell. Proteomics 22, 100663.

Kraut, R., 2011. Roles of sphingolipids in *Drosophila* development and disease. J. Neurochem. 116, 764–778.

Kumar, A., Srivastava, P., Sirisena, P., Dubey, S.K., Kumar, R., Shrinet, J., Sunil, S., 2018. Mosquito innate immunity. Insects 9.

Levashina, E.A., 2004. Immune responses in Anopheles gambiae. Insect Biochem. Mol. Biol. 34, 673–678.

Li, B., Dewey, C.N., 2011. RSEM: accurate transcript quantification from RNA-Seq data with or without a reference genome. BMC Bioinf. 12, 323.

Li, S., Yu, X., Feng, Q., 2019. Fat body biology in the last decade. Annu. Rev. Entomol. 64, 315–333.

Liu, M., Liu, L., Abbas, M.N., Kausar, S., Zhang, J.W., Ye, Z.Z., Qian, X.Y., Zhao, X.M., Chu, S.H., Dai, L.S., 2019. Involvement of gamma interferon inducible lysosomal thiol reductase in the innate immune responses of red swamp crayfish, *Procambarus clarkii*. Dev. Comp. Immunol. 99, 103405.

Lu, S., Martins, L.A., Kotal, J., Ribeiro, J.M.C., Tirloni, L., 2023. A longitudinal transcriptomic analysis from unfed to post-engorgement midguts of adult female *Ixodes scapularis*. Sci. Rep. 13, 11360.

Maya-Monteiro, C.M., Daffre, S., Logullo, C., Lara, F.A., Alves, E.W., Capurro, M.L., Zingali, R., Almeida, I.C., Oliveira, P.L., 2000. HeLp, a heme lipoprotein from the hemolymph of the cattle tick, *Boophilus microplus*. J. Biol. Chem. 275, 36584–36589.

Medina, J.M., Jmel, M.A., Cuveele, B., Gomez-Martin, C., Aparicio-Puerta, E., Mekki, I., Kotal, J., Martins, L.A., Hackenberg, M., Bensaoud, C., Kotsyfakis, M., 2022. Transcriptomic analysis of the tick midgut and salivary gland responses upon repeated blood-feeding on a vertebrate host. Front. Cell Infect. Microbiol. 12, 919786. https://doi.org/10.3389/fcimb.2022.919786.

Meister, M., Lagueux, M., 2003. *Drosophila* blood cells. Cell Microbiol. 5, 573–580.

Muta, T., Hashimoto, R., Miyata, T., Nishimura, H., Toh, Y., Iwanaga, S., 1990. Proclotting enzyme from horseshoe crab hemocytes. cDNA cloning, disulfide locations, and subcellular localization. J. Biol. Chem. 265, 22426–22433.

Nakajima, Y., Taylor, D., Yamakawa, M., 2002. Involvement of antibacterial peptide defensin in tick midgut defense. Exp. Appl. Acarol. 28, 135–140.

Nicholson, R.J., Norris, M.K., Poss, A.M., Holland, W.L., Summers, S.A., 2022. The lard works in mysterious ways: ceramides in nutrition-linked chronic disease. Annu. Rev. Nutr. 42, 115–144.

Nijhof, A.M., Balk, J.A., Postigo, M., Jongejan, F., 2009. Selection of reference genes for quantitative RT-PCR studies in *Rhipicephalus* (*Boophilus*) *microplus* and *Rhipicephalus appendiculatus* ticks and determination of the expression profile of Bm86. BMC Mol. Biol. 10, 112.

Obenchain, F.D., Oliver Jr., J.H., 1973. A qualitative analysis of the form, function and interrelationships of fat body and associated tissues in adult ticks (Acari-Ixodoidea). J. Exp. Zool. 186, 217–236.

Patel, R.T., Soulages, J.L., Hariharasundaram, B., Arrese, E.L., 2005. Activation of the lipid droplet controls the rate of lipolysis of triglycerides in the insect fat body. J. Biol. Chem. 280, 22624–22631.

Perner, J., Sobotka, R., Sima, R., Konvickova, J., Sojka, D., Oliveira, P.L., Hajdusek, O., Kopacek, P., 2016a. Acquisition of exogenous haem is essential for tick reproduction. Elife 5, e12318.

Perner, J., Provaznik, J., Schrenkova, J., Urbanova, V., Ribeiro, J.M., Kopacek, P., 2016b. RNA-seq analyses of the midgut from blood- and serum-fed *Ixodes ricinus* ticks. Sci. Rep. 6, 36695.

Perner, J., Kropackova, S., Kopacek, P., Ribeiro, J.M.C., 2018. Sialome diversity of ticks revealed by RNAseq of single tick salivary glands. PLoS Neglected Trop. Dis. 12, e0006410.

Pfaffl, M.W., 2001. A new mathematical model for relative quantification in real-time RT-PCR. Nucleic Acids Res. 29, e45.

Qin, N., Sun, H., Lu, M., Wang, J., Tang, T., Liu, F., 2020. A single von Willebrand factor C-domain protein acts as an extracellular pattern-recognition receptor in the river prawn *Macrobrachium nipponense*. J. Biol. Chem. 295, 10468–10477.

Rego, R.O., Kovar, V., Kopacek, P., Weise, C., Man, P., Sauman, I., Grubhoffer, L., 2006. The tick plasma lectin, Dorin M, is a fibrinogen-related molecule. Insect Biochem. Mol. Biol. 36, 291–299.

Seppey, M., Manni, M., Zdobnov, E.M., 2019. BUSCO: assessing genome assembly and annotation completeness. Methods Mol. Biol. 1962, 227–245.

Sheldon, T.J., Miguel-Aliaga, I., Gould, A.P., Taylor, W.R., Conklin, D., 2007. A novel family of single VWC-domain proteins in invertebrates. FEBS Lett. 581, 5268–5274.

Schwarz, A., Tenzer, S., Hackenberg, M., Erhart, J., Gerhold-Ay, A., Mazur, J., Kuharev, J., Ribeiro, J.M., Kotsyfakis, M., 2014. A systems level analysis reveals transcriptomic and proteomic complexity in *Ixodes ricinus* midgut and salivary glands during early attachment and feeding. Mol. Cell. Proteomics 13, 2725–2735.

Silva, F.D., Rezende, C.A., Rossi, D.C., Esteves, E., Dyszy, F.H., Schreier, S., Gueiros-Filho, F., Campos, C.B., Pires, J.R., Daffre, S., 2009. Structure and mode of action of microplusin, a copper II-chelating antimicrobial peptide from the cattle tick *Rhipicephalus* (*Boophilus*) *microplus*. J. Biol. Chem. 284, 34735–34746.

Simpson, J.T., Wong, K., Jackman, S.D., Schein, J.E., Jones, S.J., Birol, I., 2009. ABySS: a parallel assembler for short read sequence data. Genome Res. 19, 1117–1123.

Smith, R.C., Eappen, A.G., Radtke, A.J., Jacobs-Lorena, M., 2012. Regulation of anti-*Plasmodium* immunity by a LITAF-like transcription factor in the malaria vector *Anopheles gambiae*. PLoS Pathog. 8, e1002965.

Smith, R.C., Barillas-Mury, C., Jacobs-Lorena, M., 2015. Hemocyte differentiation mediates the mosquito late-phase immune response against *Plasmodium* in *Anopheles gambiae*. Proc. Natl. Acad. Sci. U.S.A. 112, E3412–E3420.

Sociale, M., Wulf, A.L., Breiden, B., Klee, K., Thielisch, M., Eckardt, F., Sellin, J., Bulow, M.H., Lobbert, S., Weinstock, N., Voelzmann, A., Schultze, J., Sandhoff, K., Bauer, R., 2018. Ceramide synthase schlank is a transcriptional regulator adapting gene expression to energy requirements. Cell Rep. 22, 967–978.

Sonenshine, D.E., Hynes, W.L., 2008. Molecular characterization and related aspects of the innate immune response in ticks. Front. Biosci. 13, 7046–7063.

Sonenshine, D.E., Roe, R.M., 2014. Biology of Ticks, 2 ed. Oxford University Press.

Sonenshine, D.E., Macaluso, K.R., 2017. Microbial invasion vs. Tick immune regulation. Front. Cell. Infect. Microbiol. 7, 390.

Tang, X., Metzger, D., Leeman, S., Amar, S., 2006. LPS-induced TNF-alpha factor (LITAF)-deficient mice express reduced LPS-induced cytokine: evidence for LITAF-dependent LPS signaling pathways. Proc. Natl. Acad. Sci. U.S.A. 103, 13777–13782.

Tirloni, L., Lu, S., Calvo, E., Sabadin, G., Di Maggio, L.S., Suzuki, M., Nardone, G., da Silva Vaz Jr., I., Ribeiro, J.M.C., 2020. Integrated analysis of sialotranscriptome and sialoproteome of the brown dog tick *Rhipicephalus sanguineus* (s.l.): insights into gene expression during blood feeding. J. Proteonomics 229, 103899.

Tonk, M., Cabezas-Cruz, A., Valdes, J.J., Rego, R.O., Rudenko, N., Golovchenko, M., Bell-Sakyi, L., de la Fuente, J., Grubhoffer, L., 2014. Identification and partial characterisation of new members of the *Ixodes ricinus* defensin family. Gene 540, 146–152.

Tonk, M., Cabezas-Cruz, A., Valdes, J.J., Rego, R.O., Grubhoffer, L., Estrada-Pena, A., Vilcinskas, A., Kotsyfakis, M., Rahnamaeian, M., 2015. *Ixodes ricinus* defensins attack distantly-related pathogens. Dev. Comp. Immunol. 53, 358–365.

Toprak, U., Hegedus, D., Dogan, C., Guney, G., 2020. A journey into the world of insect lipid metabolism. Arch. Insect Biochem. Physiol. 104, e21682.

Umemiya, R., Hatta, T., Liao, M., Tanaka, M., Zhou, J., Inoue, N., Fujisaki, K., 2007. *Haemaphysalis longicornis*: molecular characterization of a homologue of the macrophage migration inhibitory factor from the partially fed ticks. Exp. Parasitol. 115, 135–142.

Urbanova, V., Hartmann, D., Grunclova, L., Sima, R., Flemming, T., Hajdusek, O., Kopacek, P., 2015a. IrFC - an *Ixodes ricinus* injury-responsive molecule related to Limulus Factor C. Dev. Comp. Immunol. 46, 439–447.

Urbanova, V., Sima, R., Sauman, I., Hajdusek, O., Kopacek, P., 2015b. Thioester-containing proteins of the tick *Ixodes ricinus*: gene expression, response to microbial challenge and their role in phagocytosis of the yeast *Candida albicans*. Dev. Comp. Immunol. 48, 55–64.

Urbanova, V., Hajdusek, O., Honig Mondekova, H., Sima, R., Kopacek, P., 2017. Tick thioester-containing proteins and phagocytosis do not affect transmission of *Borrelia afzelii* from the competent vector *Ixodes ricinus*. Front. Cell. Infect. Microbiol. 7, 73.

Urbanova, V., Hajdusek, O., Sima, R., Franta, Z., Honig-Mondekova, H., Grunclova, L., Bartosova-Sojkova, P., Jalovecka, M., Kopacek, P., 2018. IrC2/Bf - a yeast and *Borrelia* responsive component of the complement system from the hard tick *Ixodes ricinus*. Dev. Comp. Immunol. 79, 86–94.

Vaibhvi, V., Kunzel, S., Roeder, T., 2022. Hemocytes and fat body cells, the only professional immune cell types in *Drosophila*, show strikingly different responses to systemic infections. Front. Immunol. 13, 1040510.

Vlisidou, I., Wood, W., 2015. Drosophila blood cells and their role in immune responses. FEBS J. 282, 1368–1382.

Voelzmann, A., Bauer, R., 2011. Embryonic expression of *Drosophila* ceramide synthase schlank in developing gut, CNS and PNS. Gene Expr. Patterns 11, 501–510.

Walther, T.C., Chung, J., Farese Jr., R.V., 2017. Lipid droplet biogenesis. Annu. Rev. Cell Dev. Biol. 33, 491–510.

Wang, Y., Zhao, S., Zhang, B., Ma, H.Y., Fang, W.H., Sheng, W.Q., Yang, L.G., Li, X.C., 2020. A novel ML domain-containing protein (SpMD2) functions as a potential LPS receptor involved in anti-Vibrio immune response. Dev. Comp. Immunol. 103, 103529.

Wasala, N.B., Jaworski, D.C., 2012. *Dermacentor variabilis*: characterization and modeling of macrophage migration inhibitory factor with phylogenetic comparisons to other ticks, insects and parasitic nematodes. Exp. Parasitol. 130, 232–238.

Wilton, D.C., Waite, M., 2002. Chapter 11 phospholipases. In: Vance, D.E., Vance, J.E. (Eds.), New Comprehensive Biochemistry. Elsevier, pp. 291–314.

Wu, J., Zhou, X., Chen, Q., Chen, Z., Zhang, J., Yang, L., Sun, Y., Wang, G., Dai, J., Feng, T., 2022. Defensins as a promising class of tick antimicrobial peptides: a scoping review. Infect. Dis. Poverty 11, 71.

Yamashita, K., Shibata, T., Takahashi, T., Kobayashi, Y., Kawabata, S.I., 2020. Roles of the clip domains of two protease zymogens in the coagulation cascade in horseshoe crabs. J. Biol. Chem. 295, 8857–8866.

Zhang, D., Du, G., 2021. Chapter 8 - phospholipid catabolism. In: Ridgway, N.D., McLeod, R.S. (Eds.), Biochemistry of Lipids, Lipoproteins and Membranes, seventh ed. Elsevier, pp. 259–280.

Zhang, Y., Xi, Y., 2014. Fat body development and its function in energy storage and nutrient sensing in *Drosophila melanogaster*. J. Tissue Sci. Eng. 6, 1000141.

Zhou, M., Abbas, M.N., Kausar, S., Jiang, C.X., Dai, L.S., 2017. Transcriptome profiling of red swamp crayfish (*Procambarus clarkii*) hepatopancreas in response to lipopolysaccharide (LPS) infection. Fish Shellfish Immunol. 71, 423–433.